University of Kentucky
UKnowledge

KWRRI Research Reports | Kentucky Water Resources Research Institute

8-1973

Enzyme and Tissue Alterations in Fishes: A Measure of Water Quality

Digital Object Identifier: https://doi.org/10.13023/kwrri.rr.68

David E. Hinton
University of Louisville

M. W. Kendall
University of Louisville

J. C. Koenig
University of Louisville

Right click to open a feedback form in a new tab to let us know how this document benefits you.

Follow this and additional works at: https://uknowledge.uky.edu/kwrri_reports


Part of the Environmental Monitoring Commons, Fresh Water Studies Commons, Terrestrial and Aquatic Ecology Commons, and the Water Resource Management Commons

Repository Citation

Hinton, David E.; Kendall, M. W.; and Koenig, J. C., "Enzyme and Tissue Alterations in Fishes: A Measure of Water Quality" (1973). *KWRRI Research Reports*. 127.
https://uknowledge.uky.edu/kwrri_reports/127

This Report is brought to you for free and open access by the Kentucky Water Resources Research Institute at UKnowledge. It has been accepted for inclusion in KWRRI Research Reports by an authorized administrator of UKnowledge. For more information, please contact UKnowledge@lsv.uky.edu.

Research Report No. 68

ENZYME AND TISSUE ALTERATIONS IN FISHES: A MEASURE OF WATER QUALITY

David E. Hinton, Ph. D.
Principal Investigator

Graduate Student Assistants:
M. W. Kendall
J. C. Koenig

Project Number A-038-KY (Completion Report)
Agreement Number 14-31-0001-3217 and -3517
Period of Project - April, 1971 - June, 1973

University of Louisville
Department of Anatomy and Water Resources Laboratory
Louisville, Kentucky

The work on which this report is based was supported in part by funds provided by the Office of Water Resources, United States Department of the Interior, as authorized under the Water Resources Research Act of 1964.

August, 1973

ABSTRACT

A variety of freshwater fishes were studied by light and electron microscopy, enzyme histochemical and biochemical methods. The objective was to determine normal structure and function in specific target organs and to compare these to altered states in aquatic pollution. The basic question, "can fish tissues and enzymes serve as indicators of water quality?," was asked. Microscopic alteration in gill was indicative of copper toxicity at an exposure of 20 parts per billion. Gross and light microscopic alterations were indicative of a single exposure of channel catfish to 15 parts per million of methyl mercuric chloride (CH_3HgCl). Microscopic and correlated biochemical study fingerprinted the alterations in cells at an exposure of 0.67 parts per million CH_3HgCl. The developments of pathobiological autopsy techniques for the assessment of water quality is discussed.

KEY WORDS:

Descriptors: Bioindicators, Biochemistry, Environmental Effects, Enzymes, Fish Physiology, Toxicity, Water Quality.

Identifiers: Fish Tissues, Fish Organs, Enzyme Histochemical Methods, Pathobiological Autopsy.

TABLE OF CONTENTS

CONTENTS

LIST OF FIGURES

LIST OF TABLES

CHAPTER I

Introduction

The primary objective of this study was to determine those alterations in fish tissues brought about by aquatic pollutants. Examination of the microanatomy of specific organ systems (gill, liver, kidney, intestine) was performed in a variety of species from unpolluted waters (i.e., those free from industrial and agricultural toxins). This phase was necessary to establish a baseline of normalcy in appraising the alterations that occur in these tissues subsequent to exposure to sublethal concentrations of various pollutants. Localization and quantification of enzyme levels in tissues was made and normal levels were compared with the levels after exposure to aquatic pollutants.

All efforts to control water pollution and ensure adequate water quality require some knowledge of the effects of pollutants upon the aquatic environment. Physical and chemical investigation of water pH, temperature, toxin concentration, dissolved oxygen, and sediment have a very great significance in this role, however, the ultimate effect of alteration in these parameters of water quality upon fish tissues is poorly understood.

Current methods for evaluating the effects of toxicants and establishing acceptable toxicant limits for fish involve ascertaining the effect

of these on the growth and reproductive capacity of the fish. Thus, extended, tedious experiments are necessary and a long period of time elapses before results are available for interpretation. Microscopic examination concurrent with enzyme histochemical studies seems better in comparison for this correlated approach offers procedures of detection of initial pathologic alteration in cells and tissues. Chemical "autopsies" on cells of fishes can be readily correlated with other data, such as those obtainable by light and electron microscopy.

In a recent review, Trump and associates[1] have sought to introduce the concept of subcellular pathology incorporating techniques of cell biology and biochemistry in the study of cellular alteration. Since this approach is similar to that employed in the present study, much of the introduction of that paper is paraphrased to explain the rationale for this study.

In order to appreciate the types of expressions of tissues to injury that occur in toxicity and disease, it is first helpful to conceptualize the cell and its modifications in injury. The differentiated cell, such as a liver parenchymal cell or a kidney tubular cell, is constantly being perturbed by its environment, which is generally harmful to the cell interior. Thus the cell is continually repairing itself in an attempt to maintain homeostasis. Cellular injury is visualized as a stimulus or

---

[1]Trump, B.F., et al., 1973. Cellular change in human disease. A new method of pathological analysis. Human Pathology, 4:89-109.

condition that perturbs homeostasis. The perturbation may be large or small and the cell may be able or unable to adapt and continue maintaining homeostasis. If homeostasis can be maintained, the injury is said to be sublethal, if it cannot, the injury is said to be lethal.

In the case of sublethal alterations, changes are commonly observed in various organelles such as the mitochondria, the lysosomes, the cell sap, the endoplasmic reticulum, the Golgi apparatus, and the nucleus.

In the case of lethal alterations, two phases of change can be recognized: the reversible phase and the irreversible phase. The reversible phase refers to alterations that occur prior to cell death and are reversible if the injurious stimulus is removed during that time. The irreversible phase refers to the changes that occur after the time of cell death; this phase is often spoken of as the phase of necrosis. During the necrotic phase the cell is converted gradually to debris, approaching equilibrium with the chemical and physical environment by processes including autolysis and denaturation.

A comparison may be made between the above processes and water quality. Clearly, poor water quality will not sustain life and would produce lethal alterations in fishes. Intermittent bouts of limited duration may stress fish and result in reversible alteration in tissues and cells characteristic of sublethal changes. Experimental models for study of sublethal changes incorporate correlation of chemical or

functional and light and electron microscopic information and have yielded valuable insights into the nature of altered cell function.

This study sought to determine how these concepts of cellular biology may be applied to the study of water resources problems such as interpretation of water quality.

CHAPTER II

Research Procedures

Fishes. Both wild species and channel catfish, purchased from a local dealer, were included in the study. In addition, water, bottom sediment, phytoplankton, zooplankton, and emergent insects were assayed for mercury content.

Wild species studied were: Carp, Threadfin shad, Buffalo, Golden red horse, White bass, Blue gill sunfish, White crappie, Longnose gar, Largemouth bass, Green sunfish, Longear sunfish, Bluntnose minnow, and Rosefin shiner. Of the above species, mercury determinations were carried out in Carp through Longnose gar and in Channel catfish. Bluegill, Green and Longear sunfish, Rosefin shiner and Bluntnose minnow were provided us by the Newtown Laboratory of the Environmental Protection Agency. These included fishes which were exposed to copper as well as control fishes from the same stream. Histologic analysis of the control and copper treated fishes was performed.

Channel catfish weighing 65-235g were purchased from a local dealer and maintained in 110 gallon glass aquaria in the University of Louisville Animal Care Facility. The aquarium water was maintained at 20-23°C or was allowed to equilibrate through open windows with

outside temperature. Water was aged, dechlorinated, aerated and continuously filtered through spun glass and charcoal.

Histologic methods. Bouins fixative, at room temperature, was experimentally determined to be more effective in preserving tissue components than the other fixatives, neutral buffered formalin, and Regaud's. Following Bouins fixation, tissues were stored in 70% alcohol until further processing could be done. Tissues studied included gill, kidney and liver in all fishes, and in addition, intestine of Channel catfish was studied. Small fish were placed in fixative and evisceration took place under the liquid surface. Larger fish were stunned with a sharp blow to the head, and their viscera rapidly dissected and placed in appropriate solutions. In all cases sufficient material from each organ was processed to permit the use of a variety of staining techniques. The amount of tissue processed and the plane of cut as well as the variety of stains resulted in sufficient sampling of materials for analysis. Following fixation, tissues were trimmed, dehydrated in alcohols, cleared in xylene and embedded in paraffin. Sections (5-8μ) were cut on an A. O. Spencer rotary microtome and mounted on glass slides for subsequent staining and viewing.

A variety of stains were employed. The analine blue collagen, periodic acid-Schiffs reagent (PAS), and reticular stains were used for the study of connective tissue. General tissue survey was performed on hematoxylin and eosin (H&E) and PAS stained material. PAS staining

was followed by a brief hematoxylin exposure to bring out nuclei. The PAS stain was used to study glycogen and mucopolysaccharide. Pretreatment of PAS stained materials with diastase permitted differentiation of glycogen from ceroid and mucopolysaccharides. Sudan IV was used to study lipid in formalin fixed material which has been frozen and sectioned with a cryostat.

Electron microscopic techniques. Both immersion and perfusion fixation were employed. Perfusion, of the entire fish, was done by inserting a cannula in the truncus arteriosus of the live fish. The cannula was quickly tied in place and a reservoir containing 50-100ml of chilled 4% glutaraldehyde in phosphate buffer, pH 7.4, was elevated to a height of 1 meter above the fish. Perfused fixative forced blood out of the heart as fixation proceeded. Fixation was followed by mincing of tissues into $1mm^3$ pieces. Tissues were postfixed in 1% osmium tetroxide and sectioned on a Sorvall MT-2 ultramicrotome. Staining was with uranyl acetate and lead hydroxide and sections were viewed on a Phillips 200 and a RCA EMU3G microscope.

For correlation between light and electron microscopic study, 1μ semithin sections were cut on a Sorvall MT-1 ultramicrotome and subsequently stained with toluidine blue or with hematoxylin and eosin.

Enzyme histochemical methods. Fresh frozen tissues were cut at 10-15μ in an International freezing microtome, affixed to precooled albuminized slides, and used for enzyme histochemical examination.

In addition, section freeze substitution techniques were used with favorable results. For the section freeze substitution method, tissues were rapidly removed from stunned fish, quenched in liquid nitrogen, stored on dry ice, sectioned on an Ames cryostat, and freeze substituted in absolute acetone at dry ice temperature (-79°C). This solution containing the tissue sections was stored on dry ice until further analysis. This technique yielded the most precise localization of acid and alkaline phosphatase enzymes.

Acid phosphatase (AcP) activity was localized using as substrate naphthol AS-BI phosphate followed by Garnet GBC diazonium salt. This combination resulted in the least diffusion. Fresh frozen sections were postfixed in 4% formalin solution for two hours at 4°C and washed in three changes of distilled water. This fixation is necessary to prevent diffusion of acid phosphatase from cells. In addition, pararosanilin combined with section freeze substitution methods resulted in very precise localization of acid phosphatase. No post fixation was required using the section freeze substitution method. Incubation time of 60 minutes at room temperature (23°C) was used in all cases. The tissues were then mounted in glycerine-jelly, glycerine, or polyvinyl pyrrolidone (PVP).

Alkaline phosphatase (AlP) activity was localized using a naphthol AS-MX phosphate with red violet LB diazonium salt. When compared to other naphthol substrates and diazonium salts, this combination of

substrate and azo dye yielded the best results. Incubation time was 1.5-3 minutes at pH 8.4.

Succinic dehydrogenase activity was localized using tetrazolium salt (Nitro-BT) and sodium succinate as substrate. Incubation time was 60 minutes and unfixed fresh frozen sections yielded the best localization and enzyme activity.

Enzyme histochemistry/electron microscopy. For this preparation, perfusion fixed liver was minced into $1mm^3$ pieces and placed in beakers containing lead acetate, B-glycerophosphate and acetate buffer at pH 5.2. Incubation was followed by treatment with a 0.5% ammonium sulfide solution. Reduced lead (black) allowed visual localization with the light microscope. The electron density of the lead was sufficient to yield precise localization of the enzyme at the ultrastructural level.

In the electron microscopic histochemistry as well as light microscopic procedures, two controls were used (heat inactivation and incubation in medium without substrate).

Atomic absorption spectrophotometric analysis. Near half-gram portions of liver, gill, kidney, gut, skeletal muscle and brain as well as whole bodies of small fishes and water, bottom sediment, emergent insects, and plankton were weighed and placed in air-tight vials containing 3ml of nitric acid. Specimens were subsequently solubilized by the addition of 3ml sulfuric acid, further oxidized by potassium per-

manganate, reduced in hydroxylamine-hydrochloride and stannous chloride and mercury levels were determined using a Coleman, Perkin-Elmer model MAS-50, flameless atomic absorption spectrophotometer.

Cell fractionation. Fish were stunned by a sharp blow to the head, weighed, measured and their livers were placed in ice-cold, 0.09M citrate buffer, pH 4.8, containing 0.25M sucrose. Except for a brief period during which the sample was weighed, all handling of tissue was done at a temperature of 0-4°C. For homogenization, tissue samples were placed in 5ml of buffer and homogenized in a glass tube using 6 passes of a pre-chilled, motordriven, teflon pestle. Homogenates were centrifuged at 1,000 X g for 10 minutes in a Lourdes refrigerated centrifuge model A-2 "Beta Fuge". Nuclear pellets were discarded and 2ml samples of the supernatant fractions were removed and rehomogenized with an equal volume of Triton X-100. The final concentration of Triton X-100 was 0.05% v/v. These samples were used for determination of total acid phosphatase activity. The remaining supernatant fraction was centrifuged at 20,000 X g for 12.5 minutes and 2ml samples of this supernatant fraction were rehomogenized with an equal volume of buffer. The pelleted fraction was resuspended in 2ml of buffer and sufficient Triton X-100 to result in a final concentration of 0.05% v/v, rehomogenized, and labelled lysosomal-mitochondrial (L&M) fraction.

Spectrophotometric methods. Enzyme activity was assayed using reagents obtained from Sigma Chemical Company. The substrate was

p-nitrophenyl phosphate disodium at a concentration of 2.0 mg/ml. Homogenates (0.2ml) were added to 1ml portions of substrate, and reactions were performed in triplicate for 30 minutes at 30°C. Final assay volume was brought to 6.2ml by the addition of 5ml of 0.1N NaOH which stops the reaction and converts the product to a colored compound. Concentrations of the product, p-nitrophenyl, were determined using a Beckman DB spectrophotometer set at a wave length of 410 nm. Triplicate protein determinations were performed using the method of Lowry et al. (1951), and enzyme activity was expressed per mg of protein.

Chemical characterization techniques. Optimum pH of hepatic acid phosphatase was determined in the following manner. The liver of a control fish was rapidly dissected and divided into six pieces. Individual pieces were homogenized in 0.09M citrate buffer with pH's from 3.5 to 6.0. The homogenates were centrifuged at 1,000 X g for 10 minutes and the nuclear pellets were discarded. Substrates were prepared using the above pH's of citrate buffer. Triplicates of enzyme activity and of protein concentration were performed in the same manner as was previously described.

To find the minimum concentration of Triton X-100 that resulted in maximum enzyme activity, the following procedure was used. Samples of post nuclear supernatant from a homogenized control fish liver were rehomogenized with various concentrations of Triton X-100. The

final concentrations of Triton X-100 ranged from 0.0005 to 3% v/v. Enzyme activity was determined as in the other experiments noted.

The energy of activation for channel catfish acid phosphatase was determined. This procedure was performed with a post nuclear supernatant fraction as follows. Samples of the supernatant fraction were transferred to assay tubes maintained at six different temperatures. Triplicate reactions were run for 30 minutes at each temperature, with the exception of the high and low temperatures where samples were removed at 10 minute intervals. Temperatures ranged from 15 to 40°C in increments of 5°C. The energy of activation was computed using the Arrhenius equation $k = Ae^{-\Delta E^{\neq}/RT}$ or $\log k = \log_e A - \Delta E^{=}/RT$, where k = the rate constant, A = Arrhenius constant, $E^{\neq}$ = energy of activation, R = gas constant in kcal/mole degree, and T = absolute temperature.

Michaelis-Menten analysis was performed on 3 samples of post nuclear supernatant fractions obtained by homogenization of channel catfish liver. Two samples of equal volume came from the supernatant of a single fish. One of these was treated with CH_3HgCl to give a final concentration of 0.037 mg/l, and the other was treated with an identical volume of buffer. The third sample was obtained from another fish, and has been stored at 0-4°C for two days. The analysis was performed in substrate concentrations which ranged from 1.666 to 0.104 mg/ml. Data from this experiment was analyzed using the double reciprocal equation of Lineweaver-Burk.

Data was analyzed with a Hewlett Packard 2,000 C time share computer using BASIC language. The data from the energy of activation experiment was analyzed using a computer program written by Dr. M. L. Dodson, Jr.

Polarographic methods (measurement of oxygen consumption). A Clark oxygen electrode mounted in a Gilson oxygraph was used to record oxygen consumption of kidney and liver supernatants. The tissue was prepared as mentioned previously, except that 0.44M phosphate buffered sucrose solution was used during homogenization. The temperature of the chamber was maintained at 23°C by the use of a jacket of circulating water pumped from a Forma refrigerator-heater unit. For each experiment there was a definite sequence for the addition of solutions into the respiratory chamber. This was done to facilitate consistent results. The respiration chamber had a volume of 1.4 ml.

The solutions pipetted into the chamber were.

1. CONTROL Solution

0.5ml	0.44M phosphate buffered sucrose
0.5ml	5mM sodium carbonate (aqueous solution)
0.4ml	Kidney or liver supernatant
1.4ml	Total

2. EXPERIMENTAL Solution

0.5ml	0.44M phosphate buffered sucrose
0.5ml	methyl mercuric chloride solution to make final concentration of 15mg/L
0.4ml	Kidney or liver supernatant
1.4ml	Total

Oxygen consumption was allowed to proceed until completion, thus establishing the total amount of oxygen consumed per mg of protein. Final recordings were given as μM of oxygen/min/mg protein.

Experimental design. In the chronic copper study fish were supplied by the Environmental Protection Agency. These fish were from Shayler Run, Newtown, Ohio, and had been exposed, for 6 to 24 months to an aqueous solution of copper sulfate at a concentration of 200 parts per billion. Control fishes were separated from the downstream treatment area by a screen of stainless steel mesh. Following streamside dissection and processing, fish were kept in fixative until further analysis in our laboratory could be accomplished. In this study, primary emphasis was placed on liver, kidney and gill.

Environmental mercury study. Three collection trips were made to the Tennessee River in western Kentucky. Below the dam forming Kentucky Lake, river water, bottom sediment, plankton, fishes and emergent insects were placed in vials containing nitric acid and transported to the laboratory for analysis of mercury content by the

previously mentioned method. Emergent insects were captured by dark lighting illumination of cloth sheets suspended from tree limbs on the river bank. This phase of the study was necessary to establish the relative tissue levels of mercury in fish from polluted streams and formed the basis for subsequent experimental concentrations of mercury in channel catfish.

Acute mercury exposure. Channel catfish, purchased from a local dealer, were maintained in our animal care facility in 55 gallon glass aquaria and 250 gallon epoxy coated tanks, tap water previously aged and dechlorinated was used. The aquaria were equipped with continuous flow filtration devices utilizing activated charcoal and spun glass. Filtered and aerated water was returned to the aquaria by plastic tubing. Control fish were maintained in a separate aquarium under the above conditions. All fish were fed a paste of beef heart, liver, and skeletal muscle or chopped chicken liver.

Experimental group 1. Methyl mercuric chloride (CH_3HgCl) was mixed in an aqueous solution of 5mM sodium carbonate. Approximately 150 fish (over the two year period) were injected intraperitoneally with 15 mg/kg body weight of CH_3HgCl (12 mg Hg/Kg). This dose level was arbitrarily selected as one with which enzyme and tissue alterations would be expected. Following injections fish were killed at 24, 48 and 72 hours and subsequently were processed for atomic absorption spectrophotometric (brain, gill, kidney, liver) enzyme histochemical

(liver and kidney), electron microscopic and biochemical (liver), and histologic analysis (liver, kidney, gill, gut).

Experimental group 2. Approximately 150 fish were injected intraperitoneally with a single dose of 1.5mg/kg body weight of CH_3HgCl (1.2mg Hg/kg). This concentration was experimentally determined to result in tissue loads of mercury within the range of concentration found in Scandinavian and Canadian fishes, and was slightly higher than that seen in the Tennessee River fishes. Volume of injected material was restricted to 1-2ml.

Control fish were injected with equal volumes of 5mM sodium carbonate which contained no methyl mercuric chloride.

Experimental group 3. This group was fed a diet containing CH_3HgCl for a period of six weeks. The experimental diet was made by thoroughly blending equal parts of beef heart, liver, and skeletal muscle. An aqueous solution containing lmg CH_3HgCl per liter was incubated and shaken with 1kg of diet for 1 hr. at room temperature. The resulting mixture was then blended in a Waring blender and random analysis revealed an average of 0.67mg Hg per g of diet. This diet was frozen in 1/2 g portions, packaged in plastic containers and fed to experimental fish at 8:00 a.m. Monday - Friday for 6 weeks. Each fish was allotted 1/2 g of diet per day. At the termination of the experiment, fish were stunned by a sharp blow to the head and pieces of liver, gill, skeletal muscle, kidney and intestine were removed and processed for morphologic study.

CHAPTER III

Results

Typical representations of microanatomy of gill, liver and kidney are shown in plates 1, 2, 3, 6 and 7 respectively.

The gill of freshwater fishes is composed of lamellae, primary and secondary. Primary lamallae were seen to contain fibrous and cartilaginous connective tissue and blood vessels (Fig. 1). Secondary lamallae, Figs. 1 and 2, were attached to a primary lamellum and were covered by an outer layer of squamous epithelium, one cell in thickness (Figs. 1-5). Immediately subjacent the respiratory epithelium, blood vessels (capillaries) were seen comprising the core of these finger-like projections. Nucleated red blood cells permitted easy demarcation of these vessels (Fig. 2). Between the tortuous vascular channels of the secondary lamellae pillar cells could be seen (Figs. 1 and 2). These were darker and larger than the blood cells and were used for support of the lamellum. Adjacent secondary lamellae were separated by clear spaces distally (Figs. 1-5) while pockets of PAS positive, mucus cells separated them at their bases (Fig. 2). Care was taken to insure uniform sites of study. In general, as one moved from the midbranchial region, toward either side, secondary lamellae became shorter and their epithelium appeared to be more

than one cell in thickness (Fig. 3). This observation has been erroneously interpreted by some to mean epithelial hyperplasia. No epithelial hyperplasia was noted in control and in copper treated fishes when gill lamellae of the midbranchial region were examined.

The liver parenchyma existed as a muralium two cells in thickness (Figs. 9 and 13). Sinusoids intervened between adjacent cords of hepatocytes (Figs. 9, 13, 14, and 15). Hepatocytes contained abundant glycogen which was red with the periodic acid-Schiff's technique (Fig. 6). Staining with hematoxylin and eosin was unsuccessful in demonstrating glycogen; thus the individual hepatocytes appeared extremely vacuolated (Figs. 7, 13, 14, and 15).

In general the PAS technique with hematoxylin to stain the nuclei was the method of choice for routine survey. The hepatocytes differed in appearance between different species and within the same species. Cells in some sections of PAS and H stained tissue were vacuolated while others (Figs. 8 and 9) revealed more cytoplasmic basophilia with fewer vacuoles. Cytoplasmic basophilia and glycogen were inversely proportioned. Wild fishes contained more glycogen per hepatocyte than did the aquarium reared fish. When lipid stains were applied to frozen sections, occasional minute droplets of intracytoplasmic fat were seen. The PAS stained, epon embedded, thick sections revealed the most glycogen (Fig. 12). Thus the contents of the hepatocytes in many of the wild fishes studied consisted almost

entirely of glycogen with a varying amount of cytoplasmic basophilia.

Nuclei (one per cell) appeared homogeneous with a prominent centrally located nucleolus. Abundant red blood cells and an amorphous acidophilic material which was slightly PAS positive were often seen in larger veins or in perivenous spaces between adventitia and surrounding parenchyma (Figs. 8 and 9). Sinusoids were well delineated by the presence of red blood cells. Walls and perivascular connective tissue of portal veins were frequently the site of pancreatic acini (Figs. 8 and 11). The apical portions of the pancreatic acinar cells revealed numerous PAS positive secretory granules. In addition, to the pancreatic tissue of portal veins, some bundles were seen (Fig. 11) in which a thick connective tissue border enclosed bile ducts, hepatic arteries, and pancreatic tissue.

The lobular pattern of hepatic parenchymal arrangement commonly seen in mammalian liver was not a finding in this study. Central veins (the initial tributaries of the hepatic veins) were differentiated from portal veins that were frequently associated with bile ducts, hepatic arteries, and pancreatic tissue (Fig. 8).

The liver connective tissue stroma was comprised chiefly of collagen and reticulum with elastic lamellae seen in some hepatic arterioles. The analine blue collagen stain revealed fibers as deep blue bands found in the hepatic capsule and in walls of vessels and bile ducts. Reticular fibers, demonstrable with the silver method were

seen in the hepatic capsule, walls of vessels and bile ducts, and in the walls of sinusoids (Fig. 10). These thin reticular fibers appeared to form a mesh pattern around hepatocytes. Pancreatic cells were separated from hepatocytes by a thin septum of connective tissue (Fig. 8). Although the majority of connective tissue within the parenchyma was of the reticular type, some broader fibers staining gray in color with the silver technique were thought to be collagen fibers.

The kidney structure within the freshwater teleosts showed no great differences in cellular detail and in general tissue organization. All kidneys were plastered against the dorsal body wall. The dorsal surface, when removed, revealed the impressions of the adjacent ribs. In addition, numerous blood vessels of the renal portal system could be seen here. These structures seemed to support the renal tissue and made dissection difficult.

Within kidneys, no zones of cortex and medulla were encountered. Rather, the organ seemed to be composed of numerous coiled tubules arranged in no apparent pattern and embedded in a matrix of hemopoietic tissue, blood vessels and fibrous connective tissue. All kidneys studied contained glomeruli (Figs. 26 and 27) within glomerular capsules. The glomerulus (Fig. 27) was seen as a tuft of capillaries fed and drained by afferent and efferent arterioles respectively, which were located 180° from the initial segment of the renal tubule. This initial portion of the renal tubule was referred to as the neck segment

(Fig. 27). At the neck segment, the flattened cells of the glomerular capsule go through an abrupt transition into the cuboidal cells lining the neck segment (Fig. 27). The luminal surface of the cells lining the neck segment were strongly PAS positive (Fig. 27) and revealed long cilia. More distally, a sharp transition to the next segment, the first proximal segment, occurred. This segment was characterized by tall columnar epithelium with a prominent PAS positive brush border (Fig. 28). In addition, numerous dark nuclei of small cells, seen between epithelial cells, were located near the tubular lumen. Further distally, gradual reduction in height of the proximal tubular cells was noted. Figure 29 reveals the appearance of the second proximal segment. This portion of the renal tubule has a low columnar to cuboidal epithelium with a brush border and very few dark nuclei. The nuclei of lining epithelium were located centrally within the cells and the cytoplasm near the cell borders was stained luch less intensely than that near the nuclei giving the tubule a banded appearance (Figs. 29 and 30). An intermediate segment followed the second proximal segment. At the proximal portion of the intermediate segment, a sharp transition was seen between the low columnar epithelium of the second proximal segment and the narrow, ciliated, intermediate segment (Fig. 30). The intermediate segment was narrower than either the second proximal segment or the next segment called distal segment. Tubular epithelium of the distal segment (Figs. 30-33) consisted of large,

rounded cells with clear cytoplasm and darkly stained adjacent cell-boarders. From the distal segment very slight changes were encountered in lining cells as the collecting duct was visualized (Fig. 33). Connective tissue laminae were seen around collecting ducts (Fig. 33).

Alterations encountered in gill sections were of the following types:

1.) a pulling away of the lining epithelium from the remainder of the secondary lamellum. This change is illustrated (Figs. 3 and 5). Nearly 100% of the copper treated fishes showed this alteration, while controls from the same stream did not.

2.) parasitic infestation. This change was encountered infrequently in wild fishes and is illustrated (Fig. 4). Usually the site was walled off by connective tissue and the central portions of the sites stained positively with PAS.

3.) hyperplasia of gill respiratory epithelium. This alteration (Fig. 6) was seen in the channel catfish following exposure to 15 mg/kg CH_3HgCl.

Hepatic alterations were seen in all mercury exposure groups although only the 15 mg/kg dosage caused extensive change. A wide variation in glycogen was noted within wild fishes studied. In those fish receiving 1.5 mg/kg CH_3HgCl, the surface of the liver was necrotic to a depth of some three to five cells thickness (Figs. 16-19). Deeper

lobules revealed no change with the 1.5 mg/kg dosage. Those fish receiving the 15 mg/kg dosage revealed a series of changes at 24, 48, and 72 hr post injection (Figs. 20-25). The initial change was a pronounced separation of the hepatic parenchyma from the portal vein with its pancreatic tissue (Fig. 21). Although similar conditions were encountered in less than optimally fixed controls (Fig. 20), this space was considered as an initial morphologic alteration in the 15 mg/kg mercury treatment group. Subsequent time periods revealed continued disruption of portal pancreatic tissue in walls of portal veins with necrosis and fibrosis (Fig. 22). Eventually central zones revealed necrosis as well (Fig. 23). By the 72 hr, the entire hepatic lobe was involved and there was near total disruption of hepatic tissue (Figs. 24-25).

Renal alterations of appreciable magnitude were encountered in all fish which received the heavier dose of methyl mercuric chloride. These are depicted in figures 34-39. Initial alterations were restricted to proximal tubule. Pulling away of lining epithelial cells was seen in the dietary and the 1.5 ppm exposure group. These changes were more apparent in the second portion of proximal tubules (Fig. 34). Higher magnification (Figs. 35-36) shows the increased number and size of cytoplasmic bodies (lysosomes and mitochondria) and pyknosis of some nuclei was encountered.

Between the 24 and 48 hr periods following the 15 ppm injection, degenerative and necrotic changes continued. Tubular epithelium was sloughed into lumina and appeared as cellular plugs (Figs. 37 and 38). In addition, basement membranes of glomerular tufts became markedly thickened and stained deeply magenta with PAS (Fig. 37). By the 72 hr, the appearance of the kidney was extremely hypocellular, and tubular casts were seen as far as archinephric ducts (Fig. 39). Kidney interstitial hemopoietic tissue was not spared. Initial alterations included an increase in PAS positive cells (macrophages). Necrosis followed this in the 15 ppm exposure group.

Histochemical localization of tissue enzymes are depicted in figs. 40-45. Acid phosphatase reaction product was localized to peribiliary canalicular sites within hepatocytes. This overlies the position of lysosomes and Golgi encountered in subsequent electron microscopic study. The reaction product, appearing as droplets is shown (Figs. 40 and 41). Glucose-6-phosphatase was restricted in liver sections to perinuclear cuffs around hepatocyte nuclei (Fig. 42). Alkaline was limited to cell membranes and brush borders of proximal tubular epithelium (Fig. 43). In many sections entire segments of renal tubule (proximal portion) were delineated by reaction product of acid phosphatase (Figs. 44 and 45). This aided the tubular differentiation studies which were described previously.

Originally the approach envisioned was one of quantification of

enzyme changes in histochemical specimens. Although superior localization was possible, these methods did not approve useful in quantifying enzymes. For this reason a correlated electron microscopic and biochemical approach was adopted after the study was well underway. The time involved in each preparatory step was greatly increased, therefore subsequent work was limited to the more promising enzyme, acid phosphatase. Techniques of ultrastructural localization and biochemical quantification and separation were employed to good advantage in the liver.

Electron microscopic study required techniques of adequate fixation. Figure 46 reveals the best fixation possible by immersion techniques. The improved fixation by perfusion is shown (Fig. 47). Perfusion fixation permitted subsequent study of all fish tissues. Endoplasmic reticulum of perfusion fixed liver cells appeared as parallel bars studded with ribosomes. Mitochondrial cristae and Golgi were seen as parallel membranes in perfusion fixed tissues. This method of whole body perfusion of electron microscopic fixative may become one of the most valuable findings in this study. This tool yields superior retention of life-like structure and permits the subsequent recognition of extremely subtle changes in response to toxins within tissues.

Normal ultrastructure of the channel catfish liver is shown in figs. 47-52. Figures 53-55 relate the alterations encountered in the acute exposure to CH_3HgCl. These included: detachment of ribosomes

from rough endoplasmic reticulum; loss of subcellular detail with large areas containing no recognizable organelles (Fig. 53); formation of microbodies (peroxisomes); loss of microvilli within bile canaliculi; increased density and irregular morphologic profiles of lipoprotein bodies; condensation and swelling of mitochondria; and an apparent increase in collagen (Fig. 55).

Ultrastructural alterations were encountered in the chronic study with channel catfish. Light microscopic study had revealed no striking differences between controls and fish fed 0.67 μg Hg/g diet for six weeks. The fine structural alterations are given in figs. 57-59. Increased cytoplasmic indentation was encountered and the hepatocytes had changed their profile to a more elongated to spindle shape. Throughout the cells increases of peroxisomes were encountered. These were often incomplete in formation with strands of endoplasmic reticulum membrane sequestering areas of medium to low electron density (Fig. 57). Mitochondrial changes were apparent and glycogen was more abundant than in the acute exposure group. An apparent increase in rough endoplasmic reticulum was present in most cells. The alterations in cellular profiles (indentation and elongation) suggested alteration in cell volume regulation (Figs. 58 and 59).

The results of five collection trips to the Tennessee River in Western Kentucky for collection of aquatic biota and subsequent mercury analysis are given in Table 1. In general, mercury levels in-

creased with ascent up the food chain. The highest levels were recorded in tissues of the top carnivores (longnose gar). Skeletal muscle and brain levels as well as the lack of aqueous Hg indicate incorporation of the organic forms of mercury and, in addition, suggest a chronic exposure. Our inability to capture channel catfish for comparison with our laboratory experiments was a sizeable deficit in this study. Subsequent studies are planned to give us a comparison between wild and aquarium reared fishes. Of general interest is the high level of Hg in the emergent insects. This may indicate that bottom organisms come into contact with sedimentable as well as organic mercury. Clearly additional monitoring of this type could indicate trends of improvement or deterioration in water quality.

Tissue concentrations of mercury from the fish studied in the laboratory experiments are given (Tables 2 and 3). In the 1.5 mg/kg exposure group, liver values increased between 24 and 48 hr post injection but returned to 24 hr values by the 72 hr. Kidney mercury remained essentially the same for the first 48 hrs followed by a decrease at 72 hrs. The intestine values paralled those of the kidney. Gill and skeletal muscle contained far less Hg and showed little or no change from day to day. In those fish receiving the 15 mg/kg dosage, 24 hr liver and kidney values were the highest followed by a sharp decrease in the 48 hr (kidney) and a plateau effect in liver. Intestine values were essentially unchanged for 48 hrs, then declined. Gill

values were highest at the 72 hr. This may indicate continued excretion by this tissue. Skeletal muscle values were nearly equal to the 1.5 values although the dosage was ten times more concentrated. Brain mercury levels increased between 24 and 72 hrs.

In an attempt to quantitate enzyme alterations in mercury toxicity, spectrophotometric procedures were used to assay hepatic phosphatase from liver homogenate. Initial characterization studies were performed and those results are given (Figs. 60-62). The optimum pH for acid phosphatase of channel catfish liver homogenate was found to be 4.0 (Fig. 60). The energy of activation of the post nuclear phosphatase fraction was 10.9 kcal/mole (Fig. 61). The rate at highest and lowest temperatures (15° and 40°C) was not limiting throughout the 30 min incubation period. Rates at the extremes of substrate concentration were constant throughout the 30 min incubation period. Post nuclear supernatant acid phosphatase had a Km of 5.22×10^{-4} mole/l., and a Vmax of 1.59×10^{-1} μ moles p-nitrophenol /hr, as determined by Lineweaver-Burk reciprocal forms of the Michaelis Menten rate equation, and a least squares computer analysis (Fig. 62). Post nuclear supernatant acid phosphatase which had been stored for 48 hrs at 0-4°C had a K_m of 6.88×10^{-4} mole/l and a Vmax of 1.22×10^{-1} μ moles p-nitrophenol/hr. The K_m of fresh post nuclear acid phosphatase, which was treated with 0.037 mg/l of methyl mercuric chloride was 1.13×10^{-3} mole/l, and the Vmax was

4.87 X 10^{-2} μ moles p-nitrophenol/hr.

In those fish receiving the 1.5 mg/kg CH_3HgCl, a significant change was found in the L and M fraction at 48 hr post injection. This activity was 1.70 X 24 hr values and 1.96 over 72 hr values ($P<0.01$ - Fig. 63).

In those fish receiving the single injection of 1.5 mg/kg CH_3HgCl, significant decreases in acid phosphatase activity were observed in all fractions at 72 hrs post injection ($P<0.05$ - Fig. 64).

CHAPTER IV

Conclusions

By proper attention to normal structure and a knowledge of the alterations occurring within tissue injury, it is possible to utilize the tissues of fishes as a sensitive measure of water quality.

Light microscopic alterations were seen in gill tissue exposed to only 20 parts per billion of copper sulfate.

Liver alterations of massive degree were seen in catfish exposed to a single dosage of 15 ppm CH_3HgCl. These were easily discernible with the light microscope and differential stains.

Lower, more subtle doses of CH_3HgCl initiated subcellular response and this organelle change was correlated with an alteration in the activity of the marker enzyme within that organelle.

Correlated electron microscopic and biochemical studies indicated the role of structure and function in water quality alteration.

The data have shown that water quality problems may be studied and assessments made by biological monitoring of the aquatic biota. Techniques of electron microscopy and cell biology narrow the number of possible variables, for many diverse toxins must eventually make their effect upon either nucleus, cytoplasm, lysosome, mitochondrion, plasma membrane, Golgi, endoplasmic reticulum or cell sap.

In addition, these studies have shed light on the mechanism of effect of change in water quality parameters. A knowledge of the effects of pollutants upon the aquatic environment is necessary before control of water pollution and adequate quantity of quality water can be achieved.

Figure 1. Gill from bluntnose minnow control fish. This section shows a branchial arch with primary lamellae attached. Cartilage is seen in branchial arch (bottom left) and in bases of primary lamellae (white arrow). Larger diameter vessel of branchial arch contains some blood cells. Secondary lamellae contain capillaries in cross section. Pillar cells (black) intervene between capillaries and connect lining epithelium of both sides. PAS & H. X200.

Figure 2. Higher magnification of gill from rosefin shiner. White arrow points to pigment in primary lamellum. This area stained positively for copper with Rubeanic acid. Large, dark arrow points to deposits of PAS positive mucus between secondary lamellae. This represents normal position and amount of mucus. PAS & H. X325.

Figure 3. Secondary lamellae near branchial arch. Note short lamellae and increased epithelium which is characteristic of this region. PAS & H. X200.

Figure 4. Encysted parasitic lesion between primary lamellae. These were frequently encountered in wild fishes. PAS & H. X160.

Figure 5. White arrows point to edematous portion of secondary lamellae. This lesion was encountered in the majority of copper treated fish. The process of one of separation of respiratory epithelium from underlying supportive tissue. PAS & H. X200.

Figure 6. Hypertrophy and hyperplasia of respiratory epithelium. This was seen in channel catfish at 48 hrs after a single intraperitoneal injection of CH_3HgCl, 15 mg/kg body weight. H & E. X450.

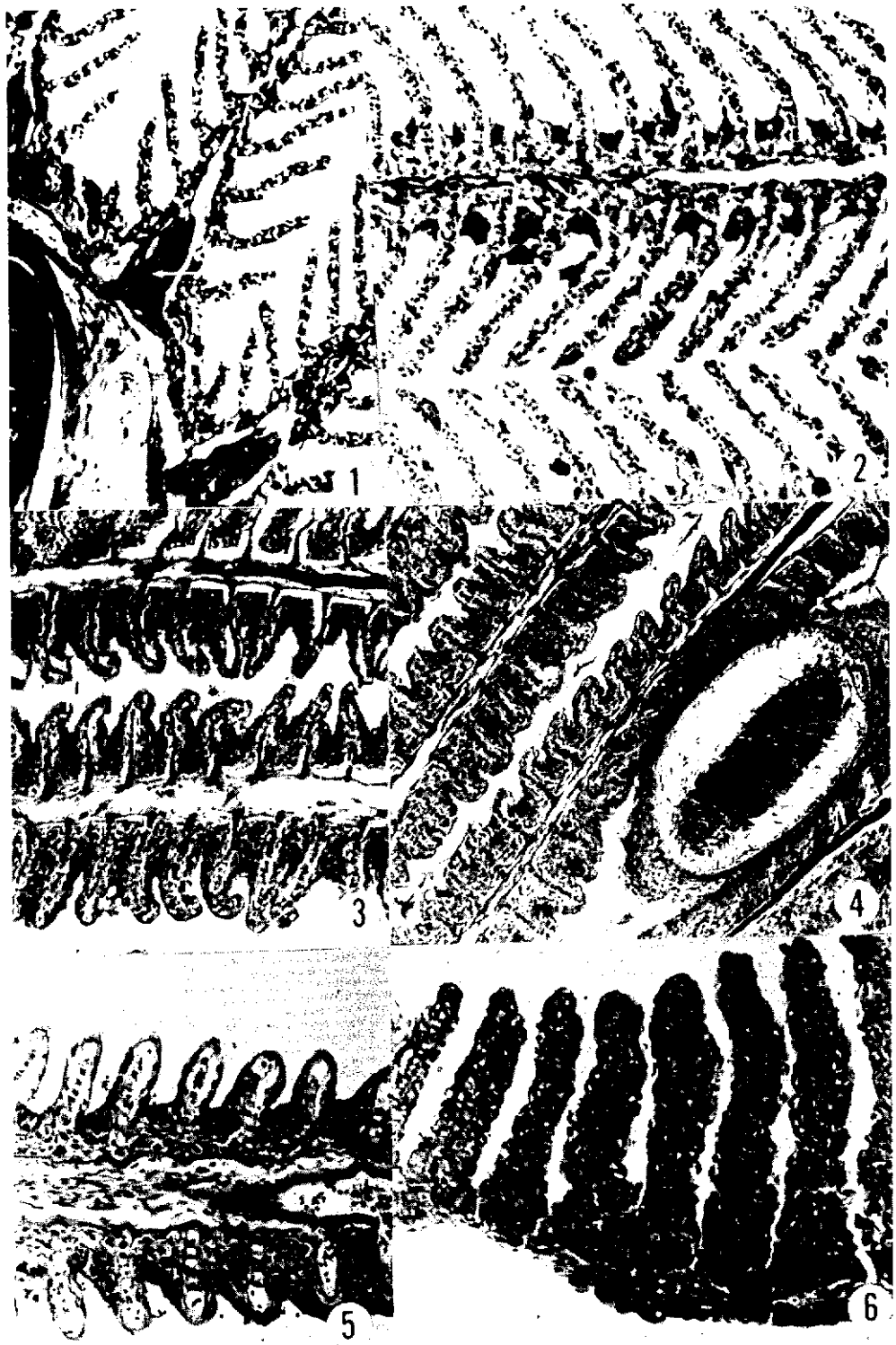
1
2
3
4
5
6

Figure 7. Extensive vacuolation of hepatocytes from wild fishes. H & E. X325.

Figure 8. Less vacuolated parenchyma of laboratory fish. Amorphous material (arrows) is in perivascular space and in vein adjacent to nucleated red blood cells. Basophilic cells in wall of portal vein are pancreatic acinar cells. PAS & H. X325.

Figure 9. Pronounced extravascular space of liver (possibly a fixation artefact) contains nucleated red blood cells and amorphous deposits (arrows). PAS & H. X400.

Figure 10. Reticular network of connective tissue in liver. Fibers delineate sinusoids and are found in walls of hepatic vessels. Silver impregnation. X325.

Figure 11. Well circumscribed bundle containing bile ducts (b), hepatic arteries (a), and basophilic cells of hepatopancreas. PAS & H. X325.

Figure 12. Nuclei (n) of hepatocytes are surrounded by dense glycogen deposits. 1 μ thick section stained with Schiff's Reagent. X950.

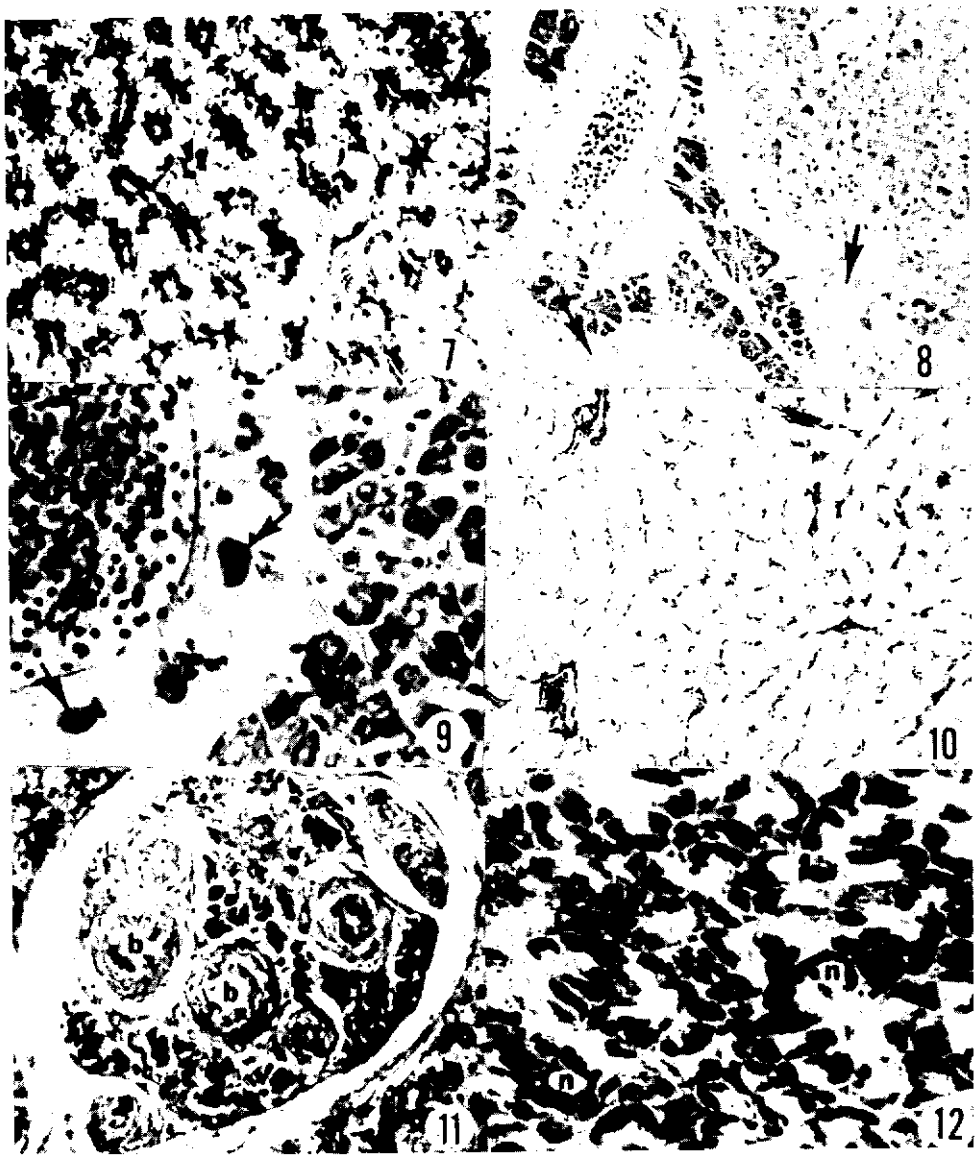
7
8
9
10
b
b
n
n
11
12

Figure 13. Dual plated muralium of cords of cells (2 cells in thickness) in which branching and anastomosing is common. This is the normal appearance of fish liver. H & E. X325.

Figure 14. A lower power view of fish liver revealing cords of cells with sinusoids intervening between adjacent cords. H & E. X200.

Figure 15. Hepatopancreas in wall of portal vein (p) appears as clumps of basophilic cells. Central vein (c) has no similar tissue. PAS & H. X200.

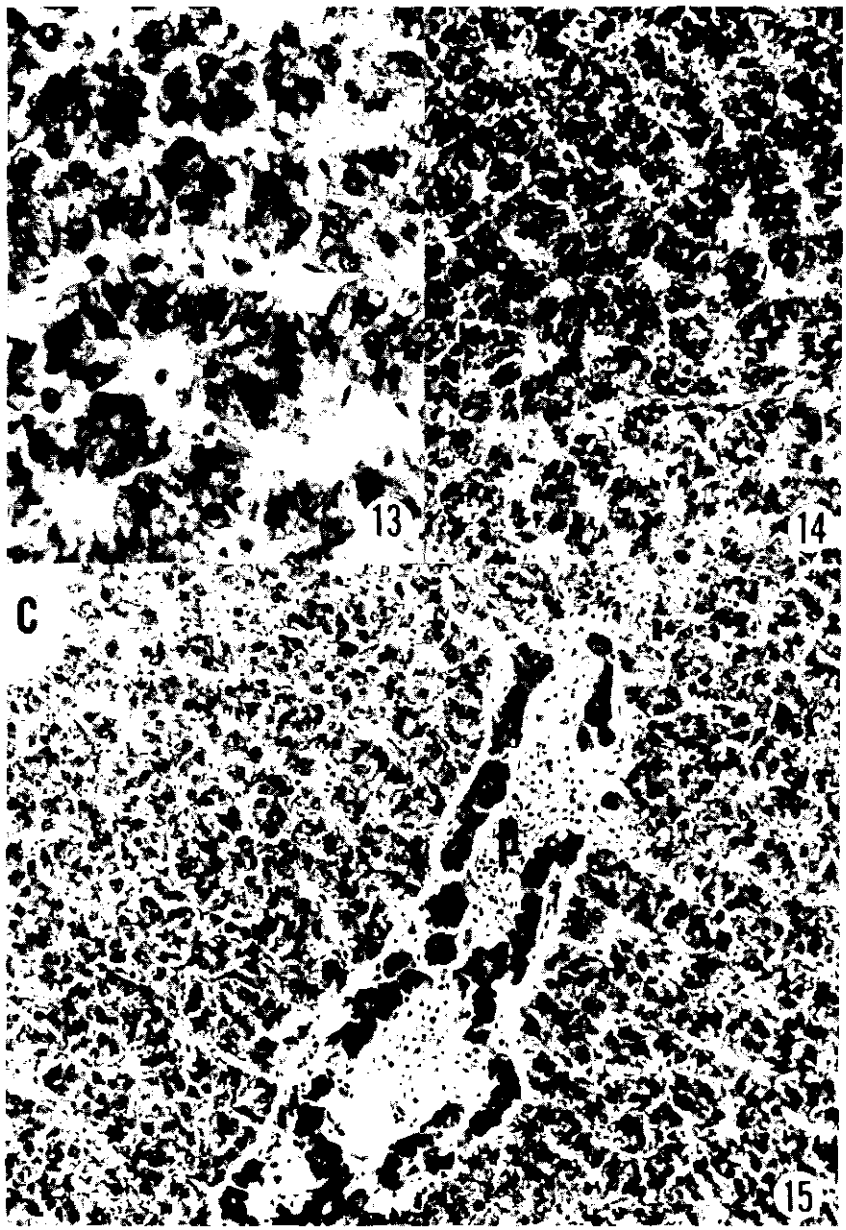
13
14
C
15

Figures 16-19 represent alterations in channel catfish liver following a single intraperitoneal injection of 1.5 mg/kg CH_3HgCl.

Figure 16. Black circle encloses subcapsular area of necrosis and hepatic cord disarray. PAS & H. X60.

Figure 17. Higher power view of area encircled (in Fig. 16) shows karolysis, pyknosis. PAS & H. X325.

Figure 18. Lower power view of liver periphery shows thickening of capsule with disarray of subjacent hepatic cords. PAS & H. X60.

Figure 19. Higher power view of figure 18 encircled area. Note thickening and increased cellularity of capsule. PAS & H. X325.

Figure 20. Normal liver reveals some extravascular space. This may be due to lack of fixation and shrinkage of tissue in alcoholic dehydration. PAS & H. X60.

Figure 21. Space same as in figure 20. Earliest change in mercury treated channel catfish was an accentuation of this space. PAS & H. X160.

Figure 22. Portal vein and pancreatic tissue reveal extensive necrosis following exposure to 15 mg/kg CH_3HgCl. PAS & H. X160.

Figure 23. Central vein and surrounding tissue from mercury treated fish reveals centrilobular necrosis with complete disorientation of hepatic architecture. PAS & H. X160.

Figure 24. Entire lobe reveals necrotic change following exposure to 15 mg/kg CH_3HgCl. PAS & H. X60.

Figure 25. Deep in affected lobe, entire section reveals necrosis of hepatic parenchyma. PAS & H. X60.

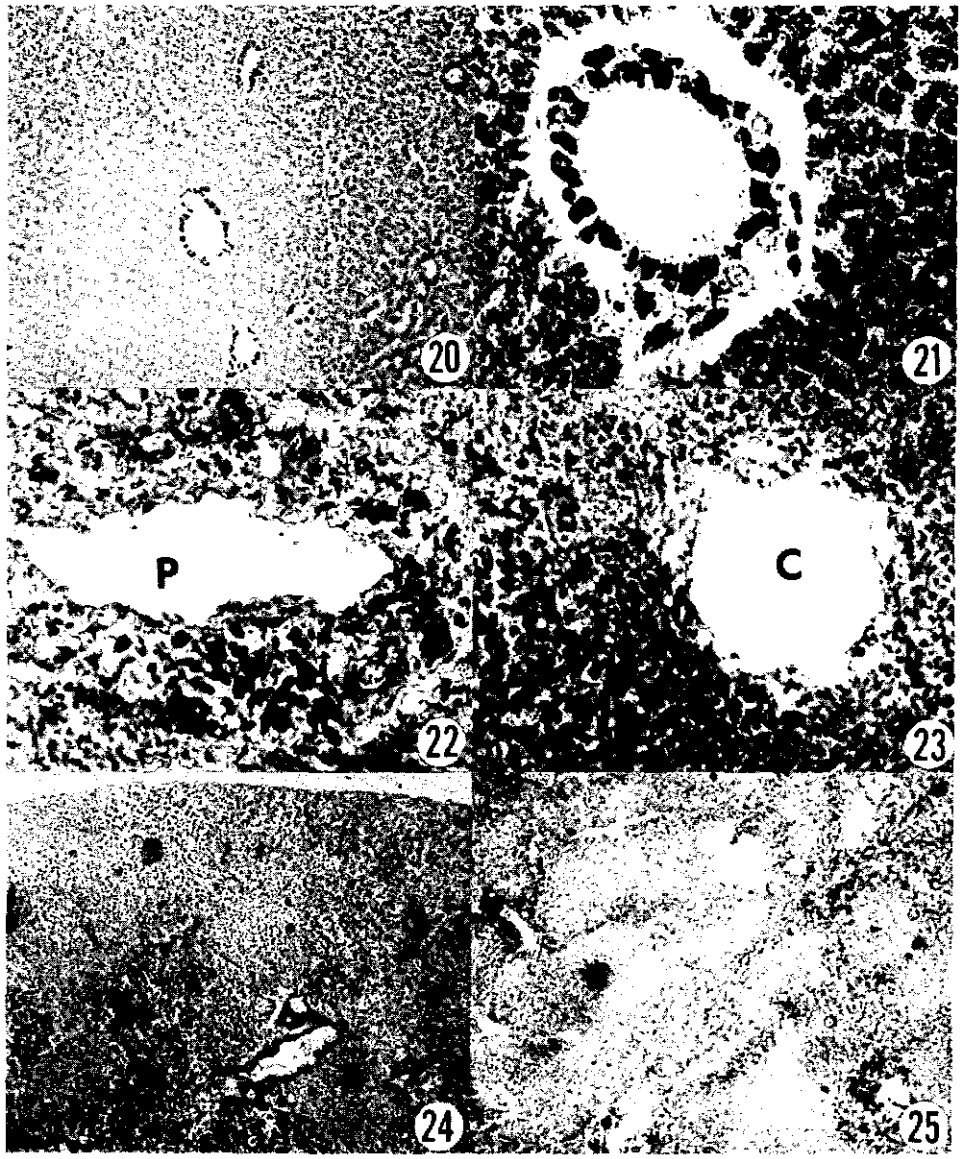
20
21
P
C
22
23
24
25

Figure 26. Normal kidney of channel catfish. Basophilic interstitial hemopoietic tissue separates renal tubules. Glomeruli (Arrow) are common. PAS & H. X400.

Figure 27. Glomerulus (G) and adjacent neck segment. Cells of glomerular capsule (arrow) are squamous while those of neck segment are low columnar and ciliated (small circle). H & E. X500.

Figure 28. First proximal segment of proximal tubule. These cells have a dense PAS + apical border and are sometimes separated by small dark nuclei (arrows). PAS & H . X500.

Figure 29. Second proximal segment of proximal convoluted tubule. This tubular segment has alternating dark (nucleus and condensed cytoplasm) and light (low density cytoplasm) bands. Pollak's polychrome. X400.


26
27
28
29

Figure 30. Second proximal segment (p) is shown as it joins the more basophilic cells of the intermediate segment (i). Next, the cloudy and swollen appearing cells of the distal segment are seen. PAS & H. X400.

Figure 31. Intermediate (i) and distal segments (d) join in this section. PAS & H. X500.

Figure 32. Junction between distal (d) segment and collecting duct (c). PAS & H. X325.

Figure 33. High magnification of junction between distal segment (d) and collecting duct (c). PAS & H. X500.


30
31
32
33

Figure 34. Segmental specificity of CH_3HgCl is shown in this section. At the 1.5 mg/kg and the 0.67 µg/g levels, these alterations were seen. There is a pulling away of the lining epithelium from the basement membrane in the second proximal segment (P_2). Some of the cells reveal pyknotic nuclei. PAS & H. X325.

Figure 35. This high magnification view of proximal tubule reveals karyolysis of tubular epithelium. Dark cytoplasmic bodies resemble lysosomes in size, amount and location. PAS & H. X900.

Figure 36. Arrow points to pyknotic nuclei of proximal tubule. PAS & H. X900.

Figure 37. Extensive loss of epithelial cells from entire kidney nephron. Glomerular basement membrane thickened. Cellular casts fill some lumina. PAS & H. X325.

Figure 38. Same as in fig. 37. Casts plug lumina of nephrons following 15 mg/kg CH_3HgCl. PAS & H. X400.

Figure 39. By 72 hrs after a 15 mg/kg injection, lesions have extended throughout nephron to collecting duct. PAS & H. X325.


P1
P2
34
35
36
37
38
39

Figure 40. Hepatic acid phosphatase. Reaction product is seen in peribiliary canalicular location. Normal amount and pattern. X325.

Figure 41. Mercury treated fish. Hepatic acid phosphatase reaction product appears as droplets somewhat larger than in controls. Sinusoids (s) are on either side of hepatic cords. X500.

Figure 42. Glucose-6-phosphatase. Reaction products appear as perinuclear cuff about nuclei (clear spots). This overlies areas of glycogen and endoplasmic reticulum.

Figure 43. Alkaline phosphatase in brush border of proximal tubule. X325.

Figure 44. Acid phosphatase in cells lining proximal tubules. X200.

Figure 45. Acid phosphatase in cells lining proximal tubules. X200.

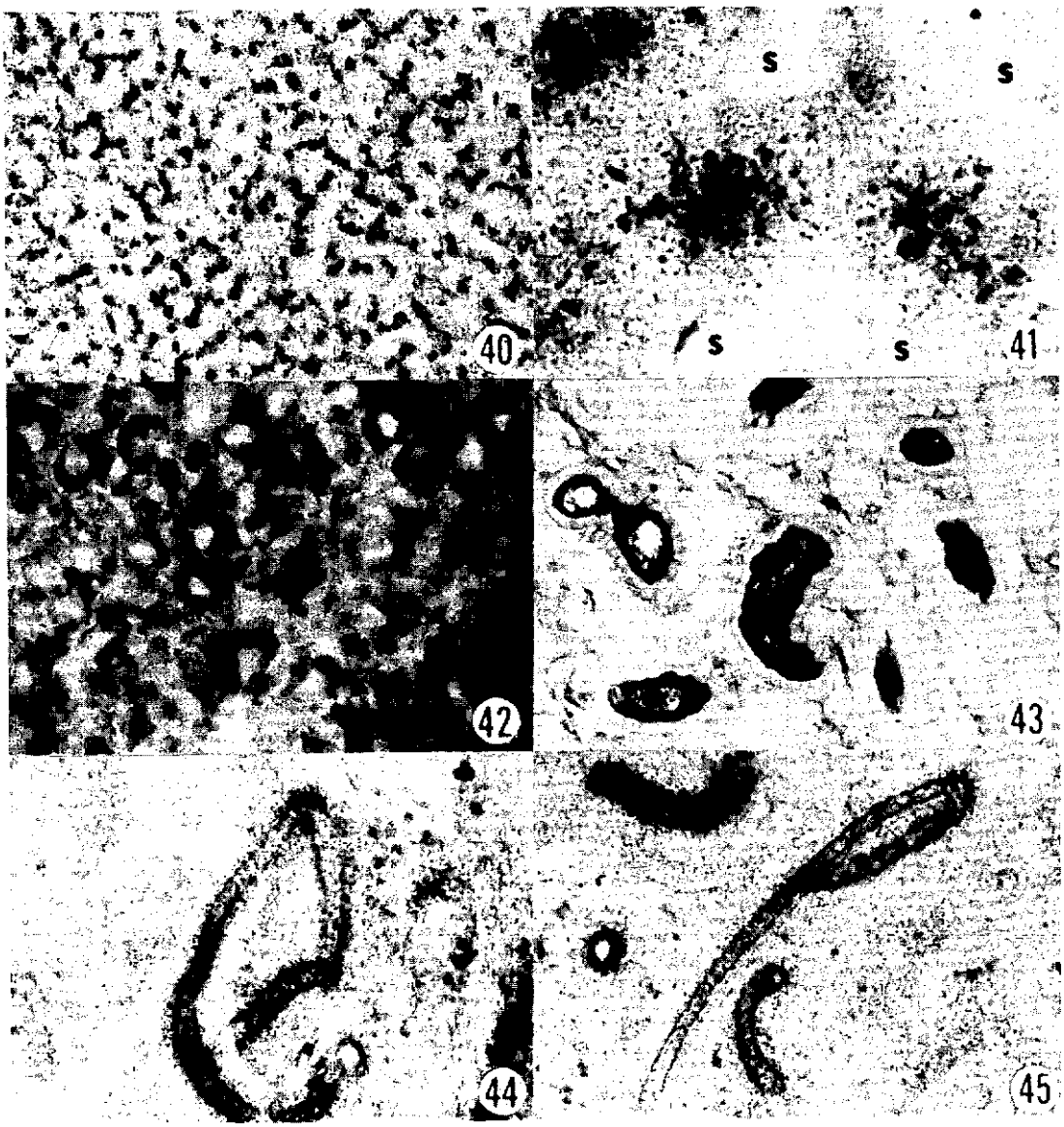
40
S
S
S
S
41
42
43
44
45

Figure 46. Immersion fixation of largemouth bass liver cell. Clumping of nuclear chromatin is associated with glutaraldehyde fixation. Note irregular cisternae of endoplasmic reticulum (er). Mitochondria (m) reveal little detail as to cristae and membranes. Glycogen (G) rosettes are not distinctly resolved. X21,150.

Figure 47. Perfusion fixation of channel catfish liver cell. Note improved overall appearance of section with better fixation. Cisternae of endoplasmic reticulum are regular and membranes are parallel. Mitochondrial cristae are easily seen. Note improved appearance of glycogen (G) rosettes. In addition, Golgi apparatus (Gol) is resolved. X17,500.

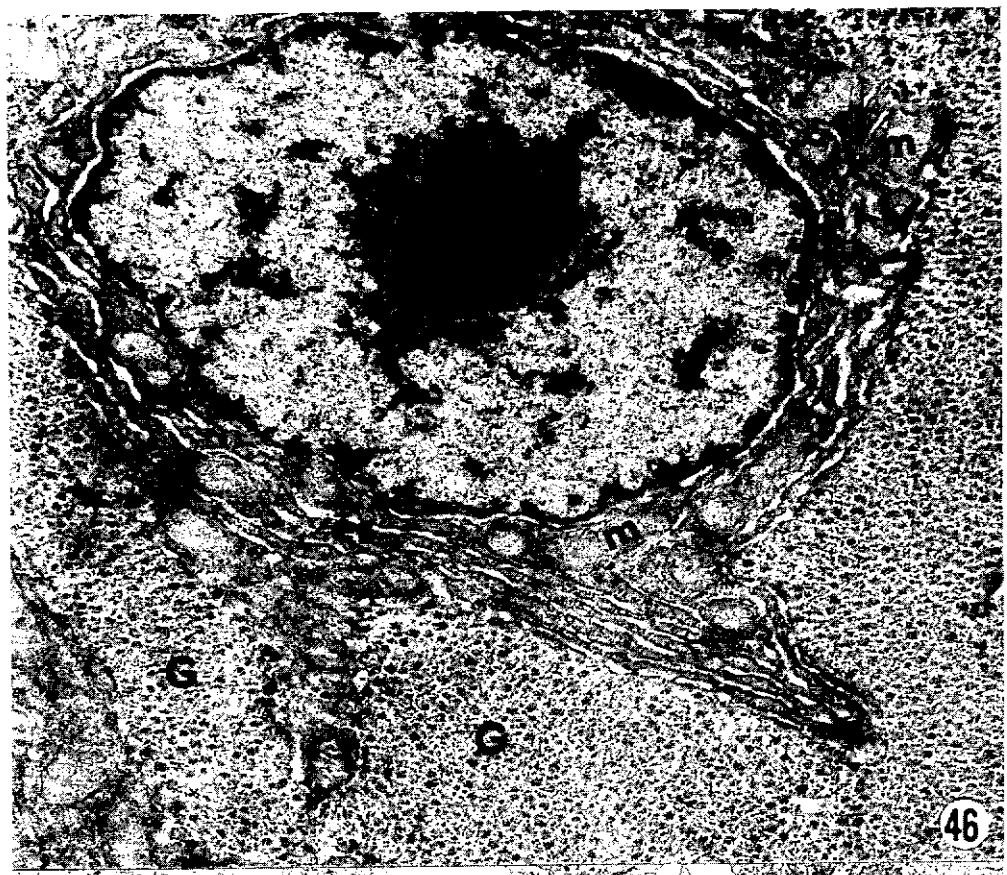
n
n
G
G
46


er
G
Gol
m
47

Figure 48. Liver, perfusion fixation of control catfish. This micrograph shows portions of 4 normal hepatocytes and a single, normal, bile ductular lining cell (at right of bile canaliculus). At center of field, microvilli of bile can be seen. This preservation is a sign of good fixation. The hepatocytes and the lining cell are attached by small, tight junctions near the bile canaliculus. Extensive Golgi apparatus is associated with numerous primary lysosomes. Pericanalicular regions in normal catfish parenchymal cells reveal spherical, oval, and angular shaped bodies. These bodies, with diameters ranging from 0.5-4 micron, exhibited structural patterns such as 1) double membrane; 2) characteristic myelin bands that appeared to be attached or fused to the inner membrane; 3) loosley arranged low density fibrillar networks; 4) disordered arrangements of medium to high density granular material; and 5) spherical to polygonal crystalline-like structures with linear dense and light areas. When micrographed under stereo angle of 9° these areas often appeared as hexagonal arrays similar to those described in artifically produced phospholipid-water systems. X17,500.

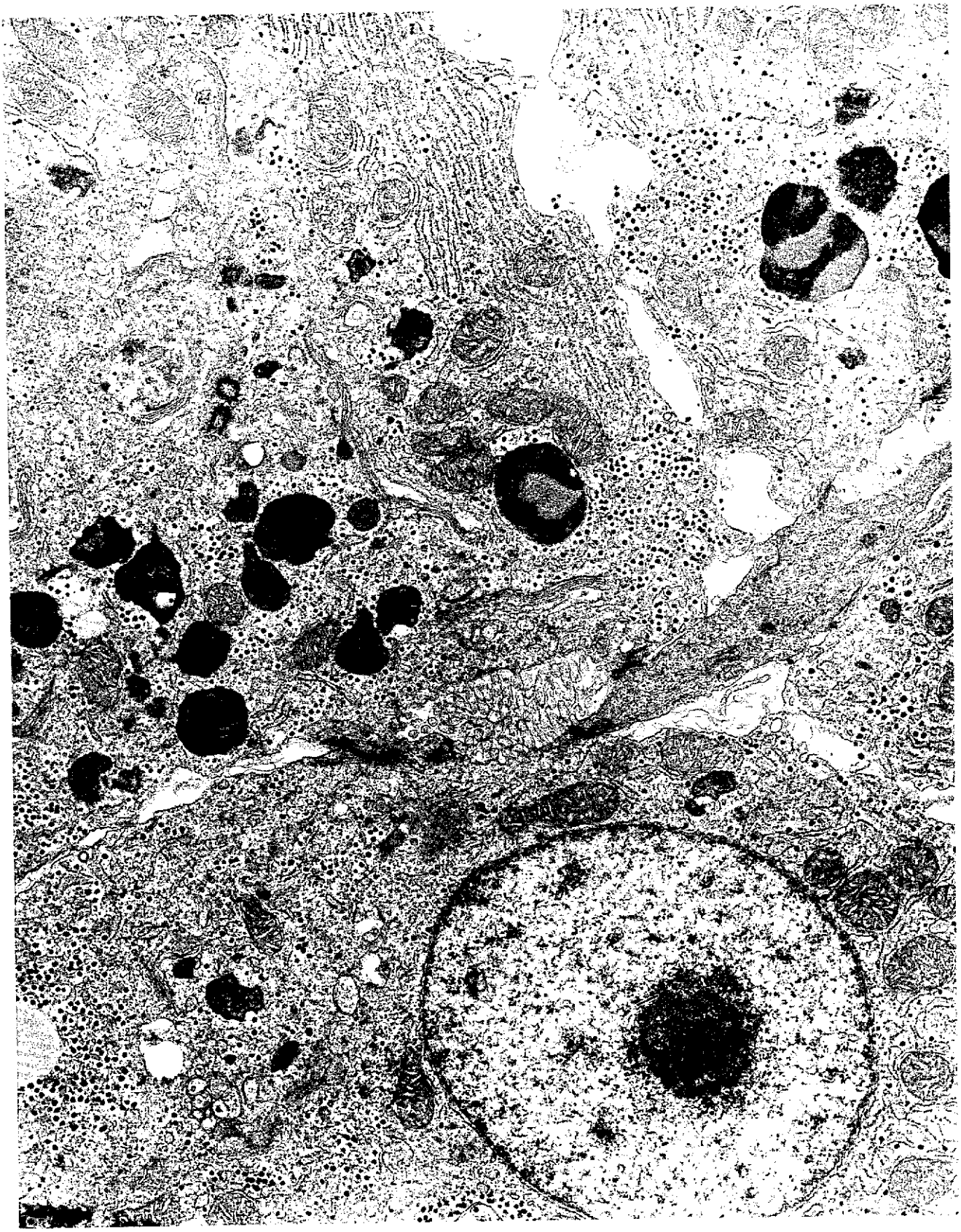

Figure 49. Liver, perfusion fixation of control channel catfish. Glycogen deposits were heavy in some control fishes. Neutral lipid (gray droplets in glycogen) occurred in close approximation to glycogen suggesting lipogenesis with glycogenolysis or the reverse. Numerous collagen is seen in the space of Disse, bottom right, between hepatocyte and endothelial cell cytoplasm. X17,500.

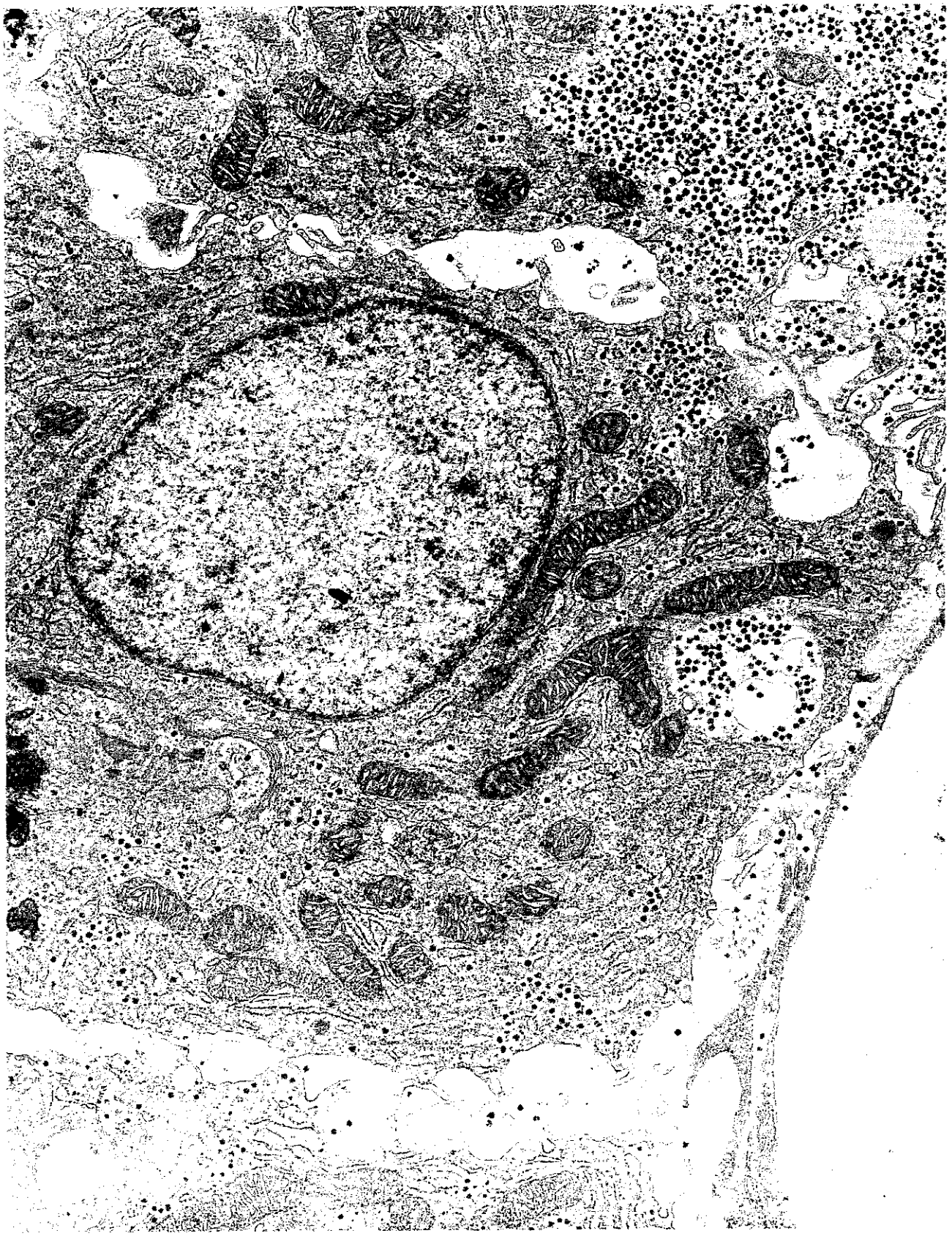

Figure 50. Liver, perfusion fixation of control channel catfish. This micrograph shows portions of 9 normal hepatocytes. Intercellular spaces are irregular due to cytoplasmic projections. Glycogen, in typical rosette pattern is seen at top of picture. Cell at center contains numerous rows of rough endoplasmic reticulum and attached ribosomes. Mitochondria are numerous and their cristae are quite apparent. Large clear space in cell at bottom left is an indentation of cytoplasm and is infrequently seen in controls. Nucleus, bottom left, reveals clumping of chromatin seen in glutaraldehyde fixation. Note single nucleolus. Cell at right, below center of page, contains abundant parallel bands of Golgi apparatus. Cytoplasmic vesicles (some of which are lysosomes) are near Golgi. Parallel array of endoplasmic reticulum, relative amount and appearance of glycogen, and cristae are evidence of good fixation. X13, 800.

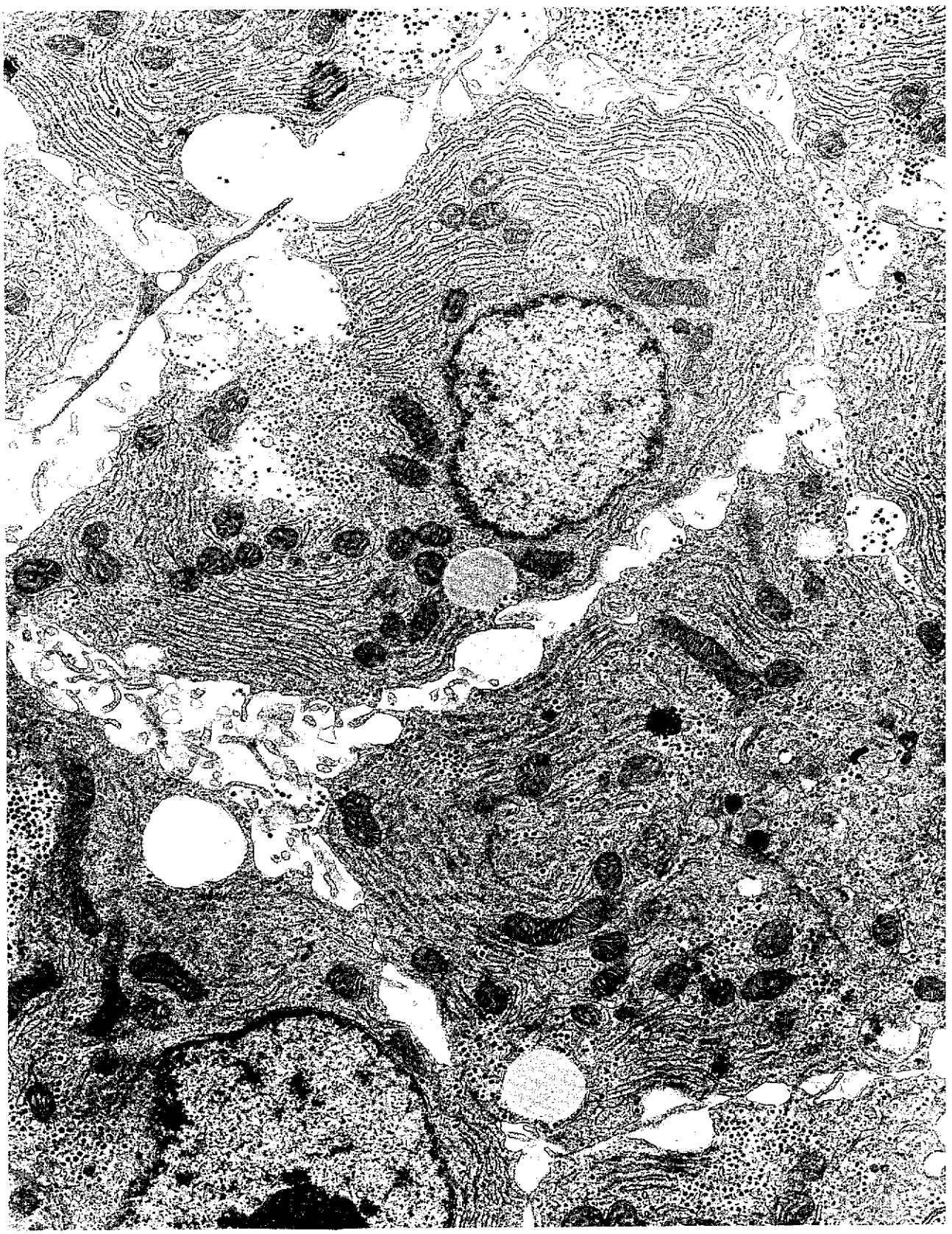

Figure 51. Liver, perfusion fixation of control channel catfish. The two cells at the top of the field are Kŭpfer cells with phagocytic function. Their nuclei are not rounded as are those of hepatocytes. Note the large amorphous mass of low to medium density material and the single membrane encircling it. This is lipofuscin. Although some similarities are seen between this and the low density fibrillar material of some lipoprotein bodies, sufficient difference exist to warrant our continued study of the lipoprotein bodies of catfish liver. X17,500.

Figure 52. Liver, control fish, perfusion fixation with 4% glutaraldehyde in phosphate buffer, pH 7.4. Lipoprotein bodies show low and high density material and have rounded to spherical appearance. Extensive Golgi faces zone of exclusion. An autophagic vacuole with circular figures of rough endoplasmic reticulum is seen at center of field. Normal appearance of catfish liver. X17,500.

Figure 53. Acute exposure to mercury in channel catfish liver. This micrograph represents the alterations seen at 24 hours after a single intraperitoneal injection of 15 mg CH_3HgCl/Kg body wt. This higher magnification reveals detachment of ribosomes from ER; irregular membranous figures associated with mitochondria (at left); and a loss of subcellular detail in bottom of field. The uneven character of the endoplasmic reticulum membranes denote alteration. Two microbodies (newly formed) in this small field indicate toxicity also.

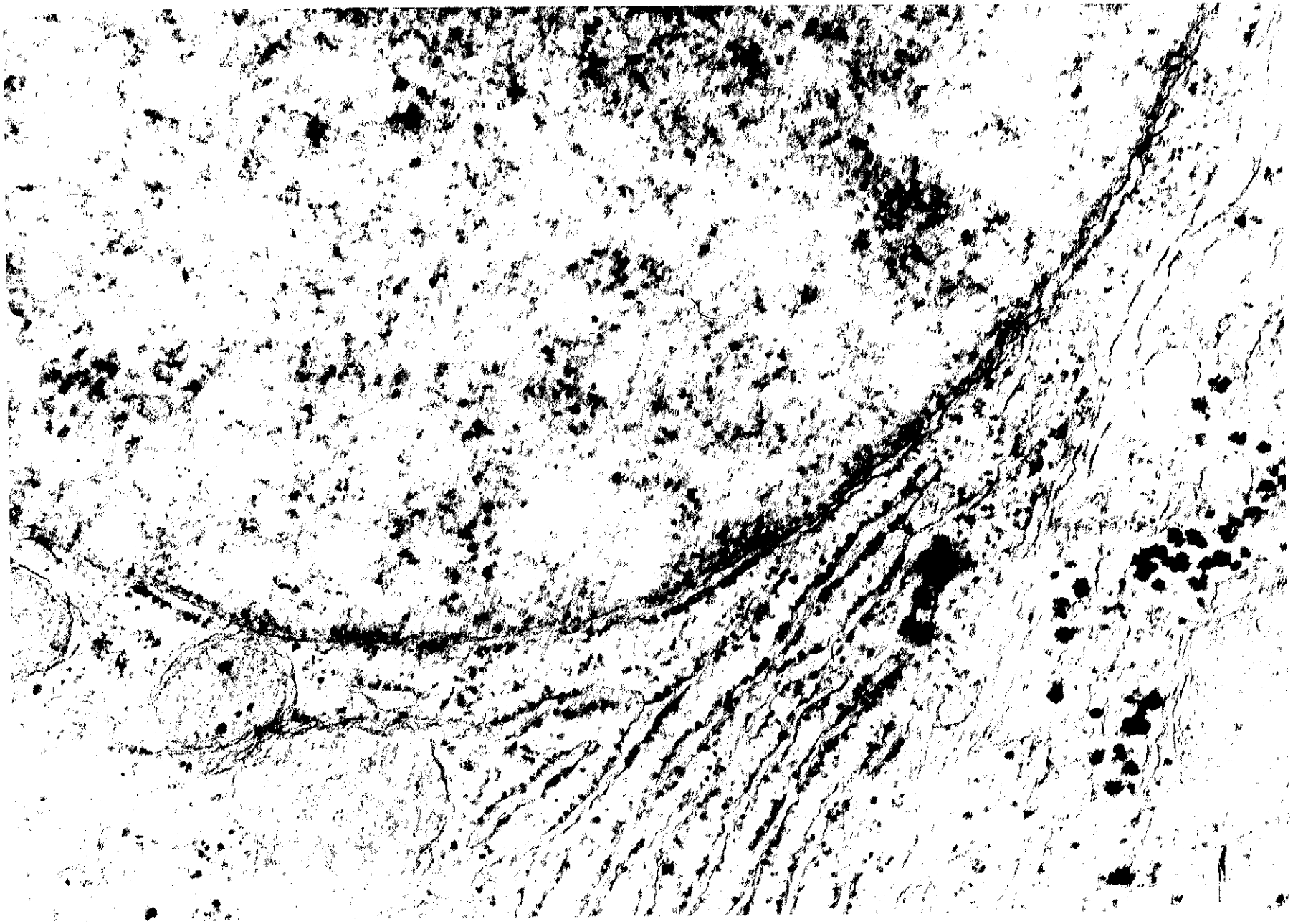

Figure 54. Acute, 24 hour, exposure to 15 ppm CH_3HgCl. Perfusion fixation with glutaraldehyde followed by post fixation in 1% osmium tetroxide. Staining was with uranyl acetate and lead citrate. Pericanalicular region of liver shows 3 altered hepatocytes and a single Küpfer cell at top left. Note near complete absence of microvilli in bile canaliculus. Increased density and irregular shape of lipoprotein bodies is apparent. Small black granular material is thought to be condensations of polyribosomes and unattached ribosomes. Mitochondria (lower left) appear swollen. Other areas reveal detachment of ribosomes from ER and dissolution of cytoplasmic vacuoles.

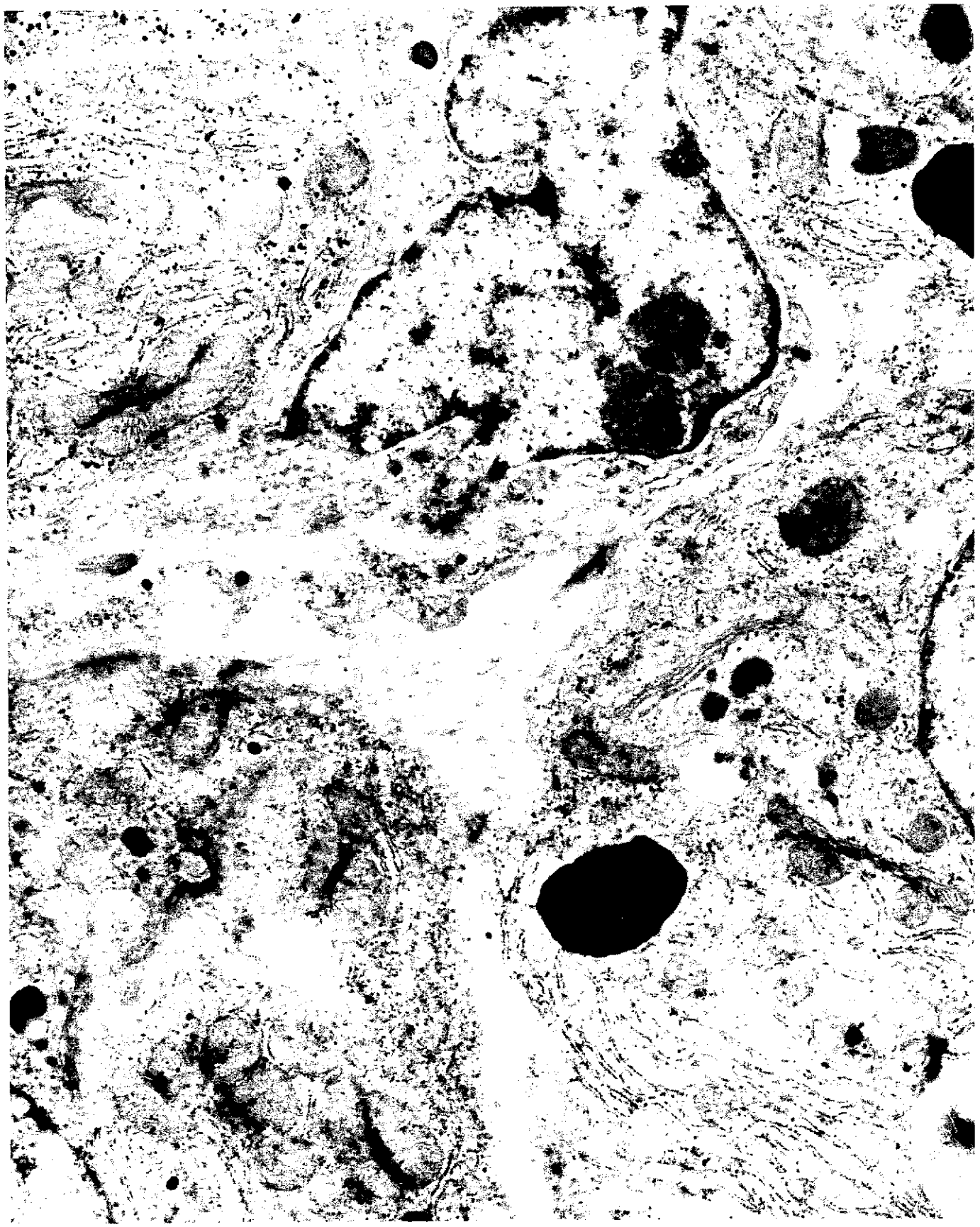

Figure 55. Acute methyl mercury exposure, liver. This lower power view shows the advanced degeneration of the cell, at center, in which numerous condensations of heavy electron density occur. Overall there is a detachment of ribosomes from RER and some mitochondria appear swollen while others have collections of membranes connecting more normal portions at either end. Collagen in this space of Disse is more than is routinely encountered.

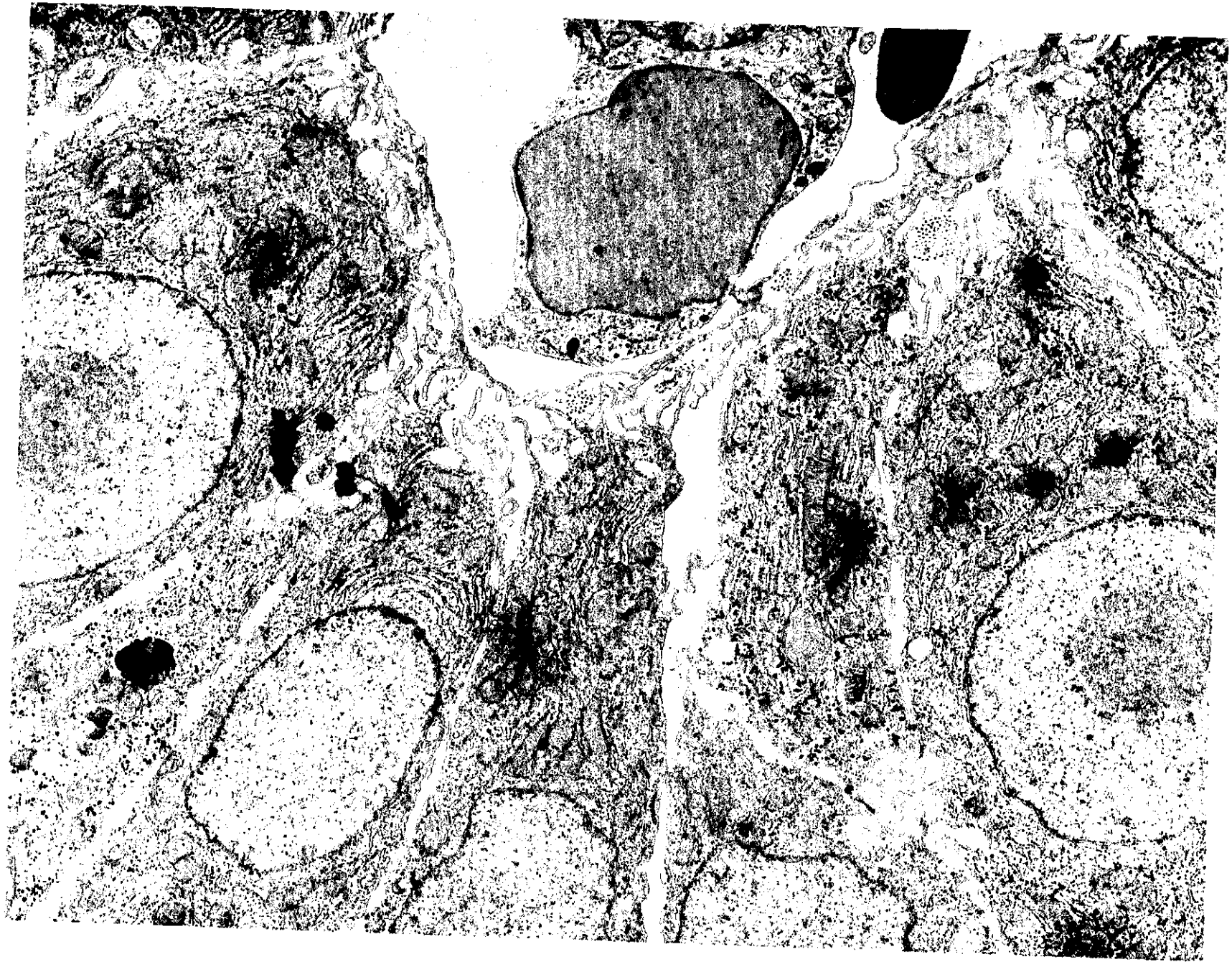

Figure 56. Acid phosphatase localization in liver of control channel catfish. Reaction product (lead phosphate) is seen over cisternae of endoplasmic reticulum, lysosomes, but not over lipoprotein bodies. Although some lysosome complexes do not contain acid phosphatase, lipoprotein bodies are thought to represent a unique continuum of membrane systems, perhaps manufactured in liver for use elsewhere. Another possibility is that of lipofuscin or ceroid pigment/residual body complex. X21,000.

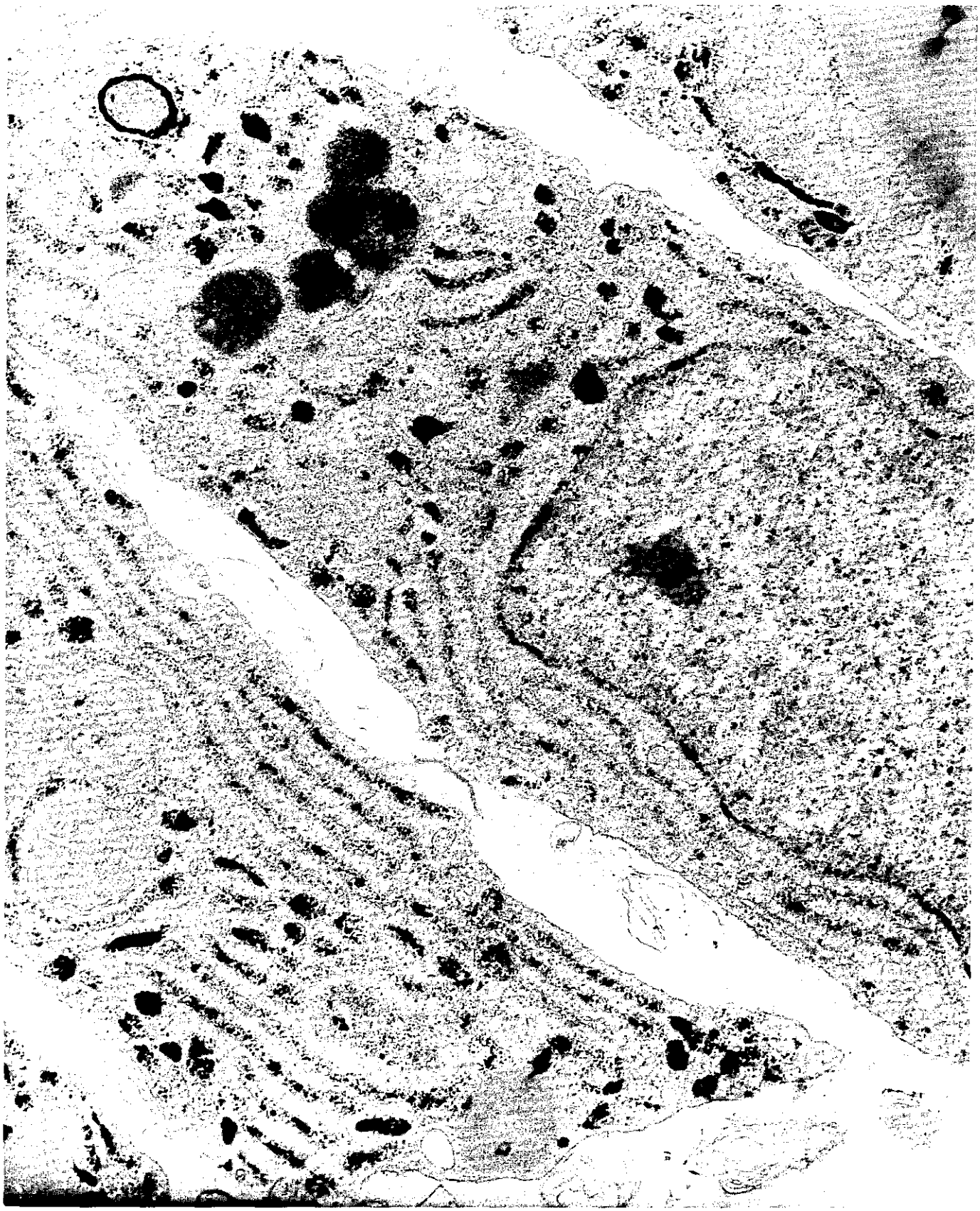

Figure 57. Liver from channel catfish dietary mercury study. Fish were fed a diet containing 0.67 µg Hg/g diet for 6 weeks. Apparent increase in rough endoplasmic reticulum is shown. In addition hepatocyte morphologic profiles have become elongated rather than polyhedral. Large cytoplasmic indentations denote other changes involving cell volume regulation. Lipoprotein bodies resemble those seen in control tissues. Numerous endoplasmic reticulum membranes are seen encapsulating areas of cytoplasm possessing medium density material. Abundant collagen can be seen in intercellular space at bottom left of field. X17,500.

Figure 58. Electron micrograph showing liver from dietary merucy experiment. Cell at upper right margin is a Küpfer cell and appears essentially normal. Its long cytoplasmic process is seen extending far along the sinusoid. The hepatocyte at top center contains lipoprotein bodies of a more electron dense character. Further down, within the same cell, areas of rough endoplasmic reticulum have been sectioned on edge. Peroxisomes throughout the entire field. X17,500.

Figure 59. This electron micrograph shows a variety of the alterations encountered in the dietary experiment. Hepatic cellular profiles are more elongated. A binucleated cell is shown at center. Increased cellular indentation is apparent. X11,500.

Figure 61. Acid phosphatase energy of activation. The slope obtained by plotting log velocity versus 1/calories equals the energy of activation.

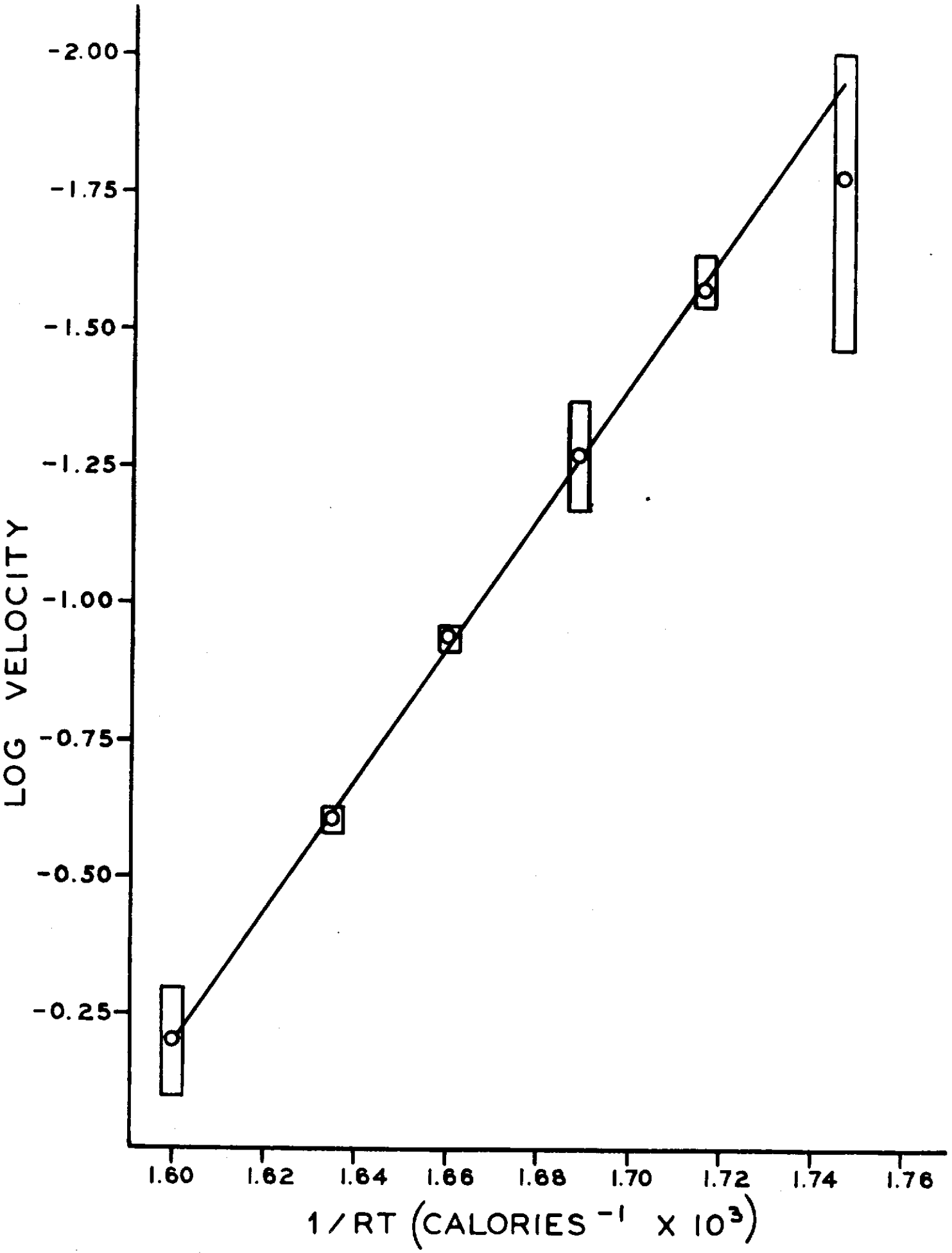
-2.00
-1.75
-1.50
-1.25
-1.00
-0.75
-0.50
-0.25
LOG VELOCITY
1.60
1.62
1.64
1.66
1.68
1.70
1.72
1.74
1.76
1/RT (CALORIES^{-1} X 10^3)

Figure 62. Effects of CH_3HgCl and storage on the Michaelis constant (intercept of 1/[s]) and maximum velocity (intercept of 1/V) of acid phosphatase. Lineweaver-Burk plot of 1/velocity (micromoles para-nitrophenol/hr) versus 1/substrate concentration. (mg/ml).

O fresh supernatant

▲ supernatant fraction stored for 47 hr at 0-4°C

● fresh supernatant fraction containing 0.037 mg/l of CH_3HgCl

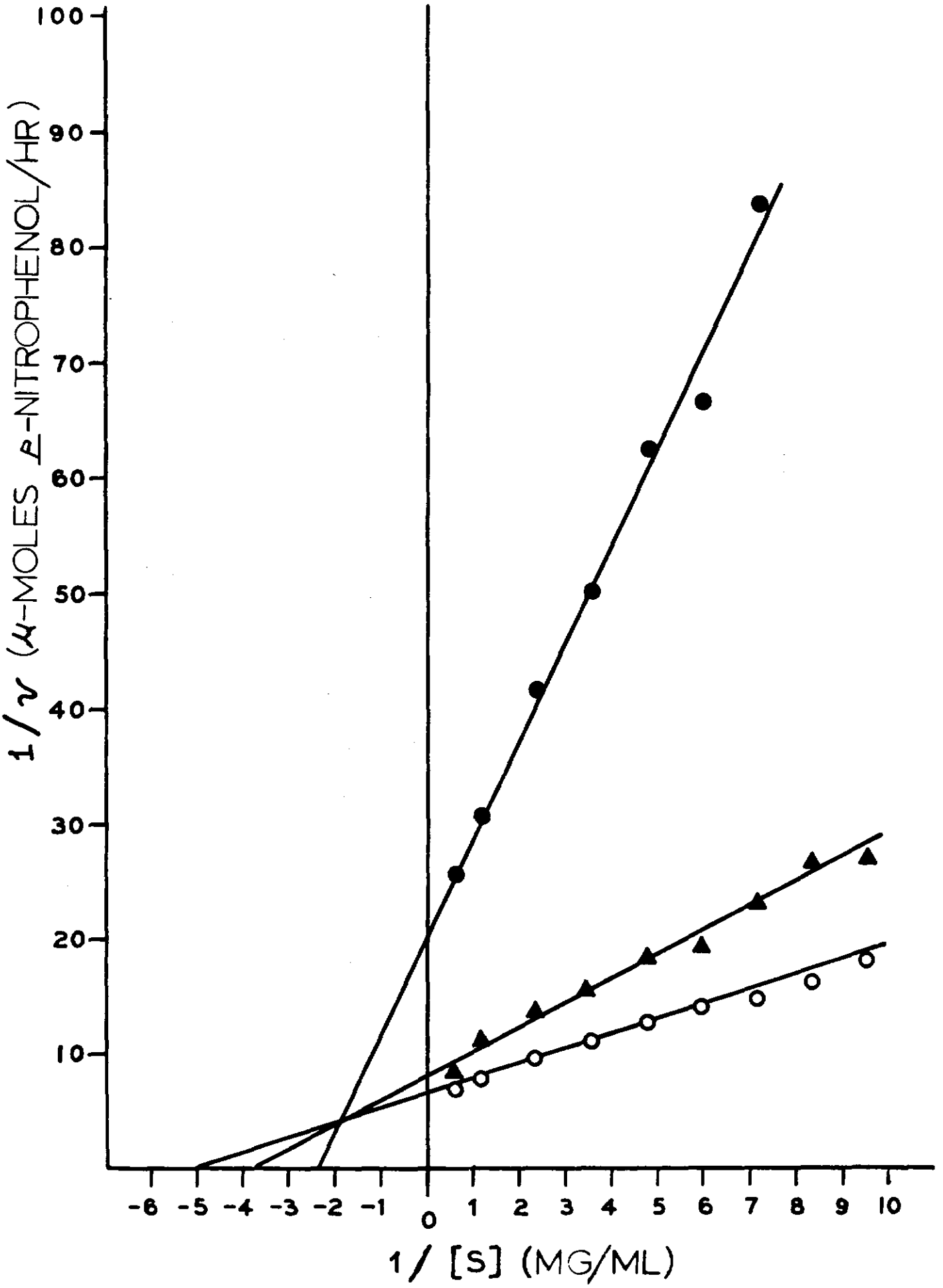
100
90
80
70
60
50
40
30
20
10
1/v (μ-MOLES p-NITROPHENOL/HR)
-6 -5 -4 -3 -2 -1 0 1 2 3 4 5 6 7 8 9 10
1/ [S] (MG/ML)

Figure 63. Specific activity of acid phosphatase in liver fractions at selected time intervals following a single intraperitoneal injection of 1.5 mg/kg CH_3HgCl. Control fish were not injected. Unless otherwise noted, each point represents triplicate determinations on 5 fish.

(A) lysosomal-mitochondrial (L&M) fraction

(B) supernatant fraction

(C) total (72 hr point based on 4 fish and 24 hr based on 1 fish)

range

95% confidence limit

● triplicate determinations on a single fish

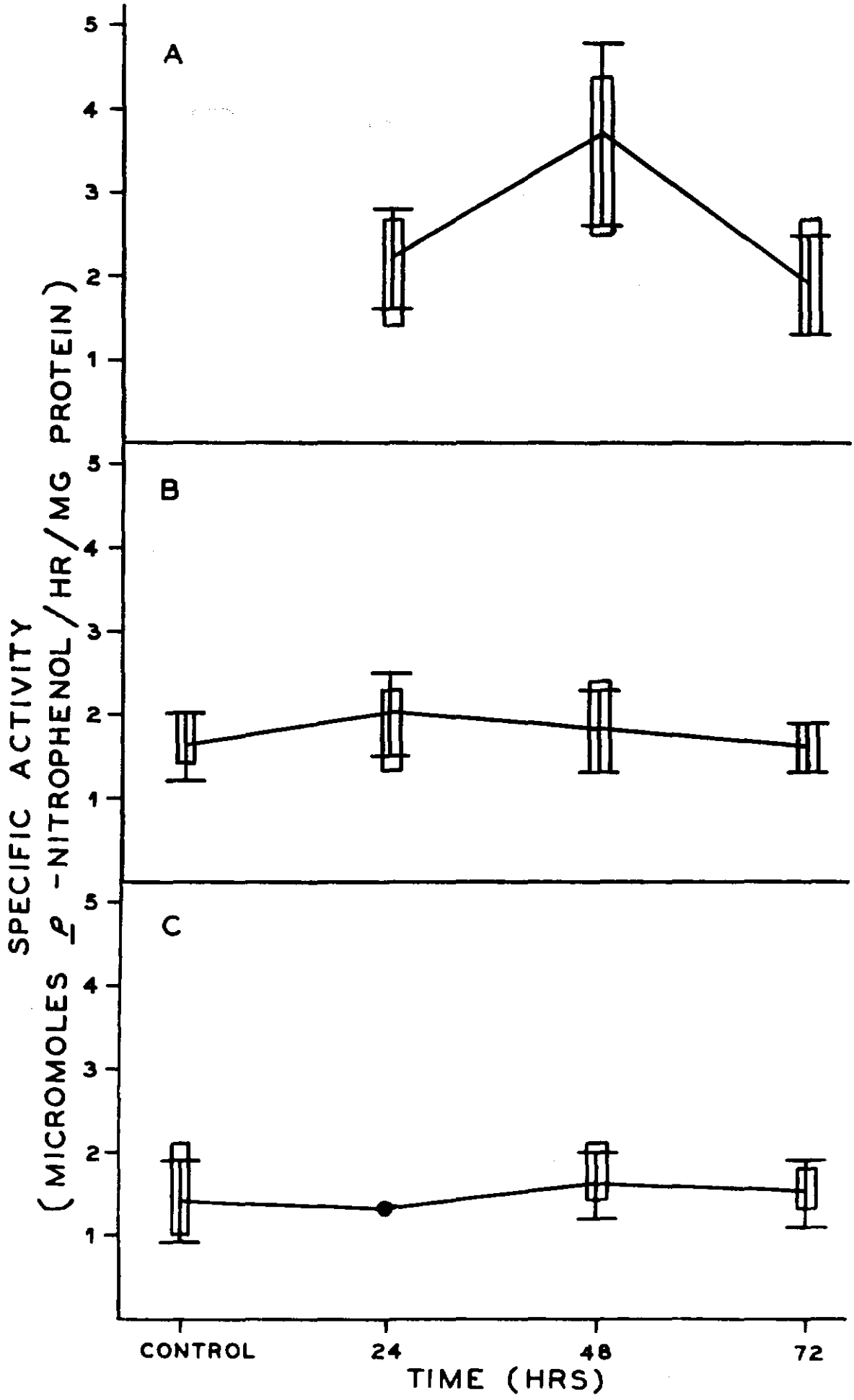
A
B
C
SPECIFIC ACTIVITY
(MICROMOLES p-NITROPHENOL / HR / MG PROTEIN)
1
2
3
4
5
CONTROL
24
48
72
TIME (HRS)

Figure 64. Specific activity of acid phosphatase in liver fractions at selected intervals following a single injection of 15 mg/kg CH_3HgCl. Control fish were sham injected. Control and 72 hr points represent triplicate determinations on 4 fish, while 24 and 48 hr points are based on 5 fish.

(A) lysosomal-mitochondrial fraction

(B) supernatant fraction

(C) total

range

95% confidence limit

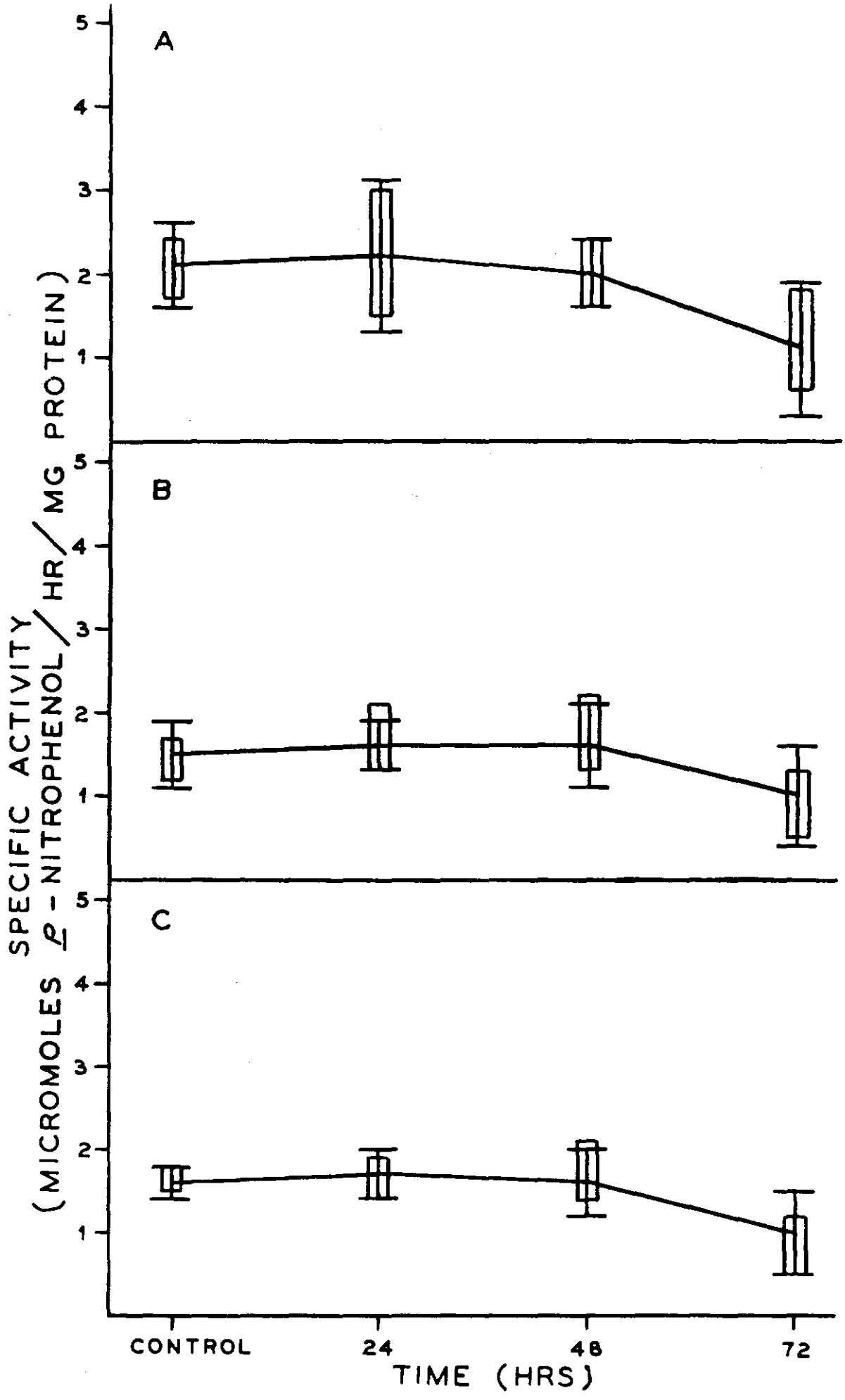
A
B
C
5
4
3
2
1
SPECIFIC ACTIVITY
(MICROMOLES p-NITROPHENOL / HR / MG PROTEIN)
CONTROL
24
48
72
TIME (HRS)

TABLE 1

MERCURY IN AQUATIC BIOTA OF TENNESSEE RIVER KENTUCKY

	ABOVE EFFLUENT	BELOW EFFLUENT
WATER	0	0
BOTTOM SEDIMENT	0.15	4.57
PLANKTON		
PHYTOPLANKTON	1.66	3.52
ZOOPLANKTON	2.2	4.14

EMERGENT INSECTS (Trichoptera) 2.05ppm

FISHES

Threadfin shad - whole body - 31 fish, 30 of 31 contained Hg
average length - 4.1cm; weight - 2.8g; Hg concentration 0.22(0.02-3.73)ppm

ORGAN ANALYSIS

	BRAIN	GILL	LIVER	KIDNEY	SKELETAL MUSCLE
THREADFIN SHAD	0.37	0.14	0.5	0.7	0.12
7 fish; 18-25cm;	0.13-0.8	0.04-0.3	0.2-1.1	0.3-1.0	0.05-0.34
CARP	1.43	0.62	0.66	1.88	0.64
2 fish; 45-46cm;	1.12-1.73	0.52-0.71	0.61-0.71	1.85-1.91	0.44-0.84
BUFFALO	0.27	0.07	0.43	0.93	0.12
1 fish; 13cm;					
GOLDEN RED	1.3	0.5	1.37	0.95	0.58
HORSE	1.2-1.4	0.46-0.56	0.9-2.3	0.7-1.2	0.4-0.7
3 fish; 31-35cm;					
WHITE BASS	0.6	0.4	0.25	0.3	0.12
7 fish; 18-22cm;	0.0-2.2	0.0-1.8	0.0-0.5	0.0-0.5	0.0-0.2
BLUEGILL	0.3	0.1	0.65	0.6	0.23
3 fish; 15-18cm;	0.2-0.4	0.09-0.14	0.3-0.9	0.0-1.5	0.22-0.24
WHITE CRAPPIE	0.7	0.13	0.5	0.49	0.4
4 fish; 23-31cm;	0.2-1.4	0.04-0.2	0.3-0.8	0.2-1.2	0.2-0.6
LONGNOSE GAR	3.7	0.7	1.9	0.88	1.2
2 fish; 61-73cm;	3.49-3.98	0.63-0.81	0.8-3.0	0.86-0.89	1.1-1.3

UNLESS OTHERWISE STATED, ALL VALUES = MERCURY IN PPM

TABLE 2

Mean Concentration (μg/g tissue) of Mercury in Organs at Selected Intervals Following a Single Intraperitoneal Injection of 1.5 mg/kg CH_3HgCl

	Liver	Kidney	Intestine	Gill	Skeletal Muscle
Controls	0.21	.24±1	.07±.03	.8±.05	.21±.1
24 hours	7.2±4	7.96±2.6	7.17±4	1.65±.8	1.18±1.2
48 hours	12.1±2	7.78±1.1	7.01±.7	1.91±.6	1.96±.4
72 hours	8±3	4.55±.6	5.21±1.4	1.61±.3	1.71±.3

± = Standard Deviation

TABLE 3

Mean Concentration (ug/g tissue) of Mercury in Selected Intervals Following a Single Intraperitoneal Injection of 15 mg/kg CH_3HgCl

	Liver	Kidney	Intestine	Gill	Skeletal Muscle	Brain
Controls	0.12	.25±.09	.26±.2	.8±12	.06±.07	0.35±.13
24 hours	87±12	51.03±15.5	18.67±6.1	8.73±.96	1.58±1.2	3.28±1.7
48 hours	78±21	38.26±6.4	16.33±4.5	9.67±2.6	1.22±1.6	4.26±.56
72 hours	65±12	39.48±4	13.70±1.9	10.87±1.3	1.67±.9	5.17±.7

± = Standard Deviation